DOI: 10.1113/JP275681

Sex-Specific Activation of SK Current by Isoproterenol Facilitates Action Potential Triangulation and Arrhythmogenesis in Rabbit Ventricles

Mu Chen[1,2], MD; Dechun Yin[1,3], MD; Shuai Guo[1,3], MD; Dong-Zhu Xu[1,4], MD, PhD; Zhuo Wang[1,5], MD, PhD; Zhenhui Chen[1], PhD; Michael Rubart-von der Lohe[6], MD; Shien-Fong Lin[1,7], PhD; Thomas H. Everett, IV, PhD[1]; James N. Weiss[8], MD; Peng-Sheng Chen[1], MD

1. Krannert Institute of Cardiology and Division of Cardiology, Department of Medicine, Indiana University School of Medicine, Indianapolis, IN.
2. Department of Cardiology, Xinhua Hospital, School of Medicine, Shanghai Jiao Tong University, Shanghai, China.
3. Department of Cardiology, First Affiliated Hospital of Harbin Medical University, Harbin, China.
4. Cardiovascular Division, Institute of Clinical Medicine, Faculty of Medicine, University of Tsukuba, Tsukuba, Japan.
5. Department of Cardiology, Renmin Hospital of Wuhan University, Wuhan, China.
6. Department of Pediatrics, Riley Heart Research Center, Indiana University School of Medicine.
7. Institute of Biomedical Engineering, National Chiao-Tung University, Hsin-Chu, Taiwan.
8. Departments of Medicine (Cardiology) and Physiology, University of California, Los Angeles, California.

Running title: Sex Differences in SK Current Activation

Keywords: ventricular arrhythmias; Ca^{2+} activated potassium channel; sex dimorphism;

Table of contents categories: Cardiovascular

For correspondence:
Peng-Sheng Chen, MD, 1800 N. Capitol Ave, E475, Indianapolis, IN 46202
Phone: 317-274-0909, Fax: 317-962-0588, email: chenpp@iu.edu

This is the author's manuscript of the article published in final edited form as:
Chen, M., Yin, D., Guo, S., Xu, D.-Z., Wang, Z., Chen, Z., … Chen, P.-S. (n.d.). Sex-Specific Activation of SK Current by Isoproterenol Facilitates Action Potential Triangulation and Arrhythmogenesis in Rabbit Ventricles. The Journal of Physiology, 0(ja). https://doi.org/10.1113/JP275681

Key Points

- It is unknown if sex difference exists in cardiac apamin sensitive small conductance Ca^{2+} activated K^+ (SK) current (I_{KAS}).
- There is no sex difference in I_{KAS} at basal condition. However, there is larger I_{KAS} in female rabbit ventricles than in males during isoproterenol infusion.
- I_{KAS} activation by isoproterenol leads to action potential triangulation in females, indicating its abundant activation at early phases of repolarization.
- I_{KAS} activation in females induces negative Ca^{2+}-voltage coupling and promotes electromechanical discordant phase 2 repolarization alternans.
- I_{KAS} is important in the mechanisms of ventricular fibrillation in females during sympathetic stimulation.

Abstract

Sex exerts large influences on cardiac electrophysiological properties. Whether sex differences exist in apamin-sensitive small conductance Ca^{2+} activated K^+ (SK) current (I_{KAS}) remains unknown. We performed optical mapping, transmembrane potential, patch clamp, western blot and immunostaining in 62 normal rabbit ventricles, including 32 females and 30 males. I_{KAS} blockade by apamin only minimally prolonged action potential (AP) duration (APD) at basal condition for both sexes, but significantly prolonged APD in the presence of isoproterenol in females. Apamin prolonged APD_{25} more prominently than APD_{80}, consequently reversing isoproterenol induced AP triangulation in females. In comparison, apamin prolonged APD to a significantly lesser extent in males and failed to restore the AP plateau during isoproterenol infusion. I_{KAS} in males did not respond to L-type calcium current agonist BayK8644, but was amplified by casein kinase 2 (CK2) inhibitor 4,5,6,7-tetrabromobenzotriazole. In addition, whole-cell outward I_{KAS} densities in ventricular cardiomyocytes were significantly larger in females than in males. Subtype 2 (SK2) protein expression was higher and CK2/SK2 ratio was lower in females than in males. I_{KAS} activation in females induced negative intracellular Ca^{2+}-voltage coupling, promoted electromechanical discordant phase 2 repolarization alternans and facilitated ventricular fibrillation (VF). Apamin eliminated the negative Ca^{2+}-voltage coupling, attenuated alternans and reduced VF

inducibility, phase singularities and dominant frequencies in females, but not in males. We conclude that β-adrenergic stimulation activates ventricular I_{KAS} in females to a much greater extent than that in males. I_{KAS} activation plays an important role in ventricular arrhythmogenesis in females during sympathetic stimulation.

Introduction

Sex is an important biological variable in cardiac electrophysiology. Females and males exhibit differences in electrocardiographic characteristics, morbidities, clinical manifestations and prognosis to cardiac electrical diseases, and drug sensitivities (Salama & Bett, 2014). For instance, women have longer corrected QT interval (QT_c) and higher incidence of Torsade de Pointes than men, while males account for a vast majority of patients with J wave syndrome (Merri *et al.*, 1989; Antzelevitch *et al.*, 2016). Rabbits have a highly matched sex-linked QT prolongation and arrhythmogenic phenotypes as in humans and are commonly used for studying the sex differences in cardiac ion channels (Salama & Bett, 2014). Previous studies in rabbits reported sex differences in several cardiac ionic currents, including the L-type calcium currents ($I_{Ca,L}$) (Sims *et al.*, 2008), the inward rectifier potassium currents (I_{K1}) (Liu *et al.*, 1998) and the rapidly (I_{Kr}) (Liu *et al.*, 1998) and slowly (I_{Ks}) (Zhu *et al.*, 2013) activating delayed rectifier potassium currents. The apamin-sensitive small conductance Ca^{2+} activated K^+ (SK) current (I_{KAS}) is abundant in atria (Xu *et al.*, 2003; Lu *et al.*, 2007; Tuteja *et al.*, 2010), sinoatrial node (Torrente *et al.*, 2017), atrioventricular node (Zhang *et al.*, 2008) and Purkinje systems (Reher *et al.*, 2017). Although SK channels are less abundantly expressed in ventricles, previous studies have demonstrated that I_{KAS} exerted important influences on repolarization and arrhythmogenicity of ventricles under pathological conditions such as heart failure (Chua *et al.*, 2011; Chang *et al.*, 2013b), myocardial infarction (Lee *et al.*, 2013; Zhang *et al.*, 2013), atrioventricular block and hypokalemia (Chan *et al.*, 2015). Due to the fact that I_{KAS} is only weakly activated under basal conditions in normal ventricles, whether or not sex differences exist in ventricular I_{KAS} activation is unknown. Sympathetic activity plays important roles in modulation of physiological fight-or-flight response as well as in cardiac arrhythmogenesis (Chen *et al.*, 2014; Shen & Zipes, 2014). Since β-adrenergic stimulation could enhance $I_{Ca,L}$ and increase intracellular Ca^{2+} (Ca_i), we hypothesized that the Ca^{2+}-dependent I_{KAS} may be activated by isoproterenol, thus allowing us to distinguish the potential sex differences. The purpose of the present study is to

test the hypotheses that there are sex differences in I_{KAS} activation during β-adrenergic stimulation, and that I_{KAS} activation plays important roles in ventricular action potential (AP) triangulation and arrhythmogenesis.

Methods

Ethical approval

All experimental procedures were approved by the Institute of Animal Care and Use Committee of Indiana University School of Medicine (IACUC no. 10961), and conformed to the Guide for the Care and Use of Laboratory Animals (National Institutes of Health).

Optical mapping

A total of 50 adult (5-6 months old) New Zealand white rabbits (26 females and 24 males) were used for optical mapping studies. We placed the rabbits in a restrainer and euthanized them by intravenous sodium pentobarbitone overdose (160 mg/kg, i.v.) before hearts removal. Hearts were harvested and Langendorff perfused with Tyrode's solution (in mmol/L: NaCl 128.3, KCl 4.7, $NaHCO_3$ 20.2, NaH_2PO_4 0.4, $CaCl_2$ 1.8, $MgSO_4$ 1.2, glucose 11.1 and bovine serum albumin 40 mg/L) that was bubbled with 95% O_2/5% CO_2 to maintain a pH of 7.40. All chemicals were purchased from Sigma-Aldrich (St. Louis, MO).

Simultaneous optical mapping of the membrane potential (V_m) and Ca_i was performed using techniques similar to that reported elsewhere (Chang *et al.*, 2013a). The hearts were stained with RH237 (10 μmol/L, from Invitrogen, Grand Island, NY) for V_m mapping and Rhod-2 AM (1.4 μmol/L, from Invitrogen, Grand Island, NY) for Ca_i mapping. Blebbistatin (15~20 μmol/L, from Tocris Bioscience, Minneapolis, MN) was used to inhibit contraction. The epicardial surfaces of right and left ventricles were excited with a laser (Verdi G5, Coherent Inc., Santa Clara, CA) at a wavelength 532 nm, and the emitted fluorescence was filtered at 715 nm long pass. The fluorescence was recorded with 100 x 100 pixels for a spatial resolution of 0.35 x 0.35 mm^2 per pixel at 2 ms/frame sampling rate. Optical signals were processed both spatially (3×3 pixels Gaussian filter) and temporally (3 frames moving average).

Seven different protocols were performed as listed below. Optical mapping data was collected at baseline and after each treatment. Protocol I was performed to test ventricular I_{KAS} at basal condition. Protocol II- IV aimed to examine if I_{KAS} is differentially activated by isoproterenol (100 nmol/L) in females and males and to determine the effects of I_{KAS} blockade on AP duration (APD) and Ca_i transient duration (Ca_iTD). Apamin (100 nmol/L) blocked I_{KAS} conducted by all SK channel isoforms while Lei-Dab7 (20 nmol/L), a highly specific SK subtype 2 (SK2) blocker, differentiated I_{KAS} conducted by SK2 from that conducted by other isoforms. Chromanol 293B (I_{Ks} blocker, 10 μmol/L) was used to exclude the effects of I_{Ks} activation during β-adrenergic stimulation. Protocol V and VI aimed to investigate the mechanisms underlying sex differences of I_{KAS}. Previous studies found that casein kinase-2 (CK2) interacted with SK2 channels and diminished I_{KAS} in neurons (Pachuau *et al.*, 2014). Therefore, we used a CK2 specific inhibitor 4,5,6,7-Tetrabromobenzotriazole (TBB, 10 μmol/L) to determine if CK2 inhibition can increase I_{KAS} in males. BayK8644 ($I_{Ca,L}$ agonist, 1 μmol/L) was applied to examine the effects of $I_{Ca,L}$ on I_{KAS} activation. Protocol VII was performed to determine the effects of I_{KAS} activation and blockade on ventricular arrhythmogenicity and ventricular fibrillation (VF) dynamics.

Since ventricular pacing and atrioventricular node ablation could activate I_{KAS} and induce short-term cardiac memory in normal rabbit ventricles (Chan *et al.*, 2015), we avoided ventricular pacing in Protocol I-IV and VI for APD measurement. In Protocol I, we optically mapped the ventricles with right atrial (RA) pacing at cycle length (PCL) 200 ms, 250 ms and 300 ms. Since isoproterenol markedly accelerated the sinus rhythm to about 240-290 beats per minute, in Protocol II-IV, we optically mapped the ventricles at a fixed atrial PCL 200 ms in order to reach 1:1 capture. Optical mapping data in Protocol V and VII were collected under ventricular pacing. However, to minimize the ventricular pacing induced I_{KAS} activation, we left the ventricles unpaced except during induction of cardiac alternans and VF. In all protocols, the agents were sequentially added to the perfusate and recirculated until washout.

Protocol I: Baseline- apamin- washout in 3 females and 3 males. After baseline mapping, apamin was added to the perfusate. We then waited 15 minutes to collect post-apamin optical mapping data.

Protocol II: Baseline- isoproterenol- apamin- washout in 8 females and 8 males. After baseline mapping, the heart was perfused with isoproterenol for 10 minutes before the data

collection. Apamin was then added to the perfusate while isoproterenol was kept in recirculation. During the washout, isoproterenol can be completely washed out while apamin cannot be fully washed out.

Protocol III: Baseline- isoproterenol- Lei-Dab7- apamin- washout in 4 females. Lei-Dab was administered while isoproterenol was recirculated in the perfusate. Data collection was performed 10 minutes after Lei-Dab administration.

Protocol IV: Baseline- chromanol 293B- isoproterenol- apamin- washout in 4 females and 3 males. Chromanol 293B was pretreated for 30 minutes before isoproterenol administration and kept in the perfusate until washout.

Protocol V: Baseline- TBB- apamin- washout in 3 males. TBB was perfused for 15 minutes before data collection and was recirculated until washout.

Protocol VI: Baseline- BayK8644- apamin- washout in 3 females and 3 males. BayK8644 was perfused for 15 minutes before data collection and kept in perfusate until washout.

Protocol VII: Baseline- isoproterenol- apamin- washout with ventricular pacing in 4 females and 4 males. In this protocol, RV pacing at PCL 150ms was performed to induce cardiac alternans. RV burst pacing (PCL 50 ms, duration 10s) was used to induce VF. VF induction was attempted 10 times at baseline and after each treatment. Any VF occurrence was allowed to continue for 2 minutes before electrical defibrillation. We optically captured the first 100 ms at the initiation of VF. Maps of phase singularities (PS) and dominant frequency were also performed. The PS number was manually counted at each time point separated by 10 frames (20 ms) of data (Hayashi *et al.*, 2007). Pseudo-electrocardiograms (pECG) were simultaneously monitored throughout the entire experiment with widely spaced electrodes in the tissue bath.

Transmembrane Potential Recording

To verify the optical mapping findings at cellular level, we performed transmembrane potential (TMP) recording of cardiomyocytes from the epicardium of LV base using the protocol of baseline- isoproterenol- apamin- washout in 4 hearts (2 females and 2 males). After immobilization of the Langendorff-perfused hearts by blebbistatin, standard glass capillary microelectrodes filled with 3 mol/L KCl with a tip resistance of ≈20 MΩ at the digitization rate of 10 kHz was used to record TMP. The data was stored with Axoscope 10.2 (Axon Instrument, Inc). Experiments were performed at 38.3 °C.

Ventricular cardiomyocytes isolation

Ventricular cardiomyocytes were isolated from an additional 8 rabbits (4 females and 4 males) for the use of patch clamp, western blot and immunostaining studies. After intravenous sodium pentobarbitone overdose, hearts were quickly excised by thoracotomy and Langendorff perfused for 5 min with Tyrode's solution followed by perfusion with a oxygenated buffer containing (in mM): 138 NaCl, 5.4 KCl, 0.3 NaH_2PO_4, 1.2 $MgCl_2$, 10 HEPES, 10 taurine and 10 glucose (pH 7.4 with NaOH at 37 °C). This was followed by 15 min perfusion with the same buffer containing 1 mg/ml collagenase (Type II, 270 U/mg; Worthington) and 0.1 mg/ml protease (Type XIV, ≥3.5 U/mg; Sigma). The heart was removed from the Langendorff apparatus. Cardiomyocytes from the base of the left ventricles were dissociated from digested ventricles by gentle mechanical dissociation.

I_{KAS} densities determined by voltage-clamp techniques

Voltage-clamp experiments were conducted at room temperature. Axopatch 200B amplifier and pCLAMP-10 software (Axon; Molecular Devices, Sunnyvale, CA) were used to generate and record all patch experiments. Pipette electrodes were fabricated using Corning 7056 glass capillaries (Warner Instruments).

For whole-cell I_{KAS} measurements, the pipette solution contained (in mmol/L): potassium gluconate, 144; MgCl2, 1.15; EGTA, 5; HEPES, 10; and $CaCl_2$ yielding a free (unchelated) [Ca^{2+}] of 1 μmol/L (pH 7.25 using KOH). The extracellular solution contained (in mmol/L): N-methylglucamine, 140; KCl, 4; $MgCl_2$, 1; glucose, 5; and HEPES, 10 (pH 7.4 using HCl). The voltage-clamp protocol consisted of ramp-pulse protocol (test pulse: between +40 and -120 mV, holding potential: -70 mV; pulse frequency: every 3 seconds). Pipette resistance ranged from 1 to 2 MΩ. Series resistance was electronically compensated by 70% to 80%. Currents were recorded at baseline and after the exposure to 100 nmol/L apamin. We also recorded the current in the presence of 100 nmol/L isoproterenol and after apamin. To obtain whole-cell I_{KAS}, currents recorded in the presence of 100 nmol/L apamin were digitally subtracted from those recorded in its absence.

To verify the selectivity of Lei-Dab7 for I_{KAS} conducted by SK2 but not SK3, we tested the effects of Lei-Dab7 on human embryonic kidney (HEK) 293 cells transfected with *KCNN2* and *KCNN3*, respectively. HEK 293 cell were cultured in Iscove's Modified

Dulbecco's Medium (Gibco) with 10% fetal bovine serum and 1% penicillin/streptomycin in 5% CO_2 at 37°C. 35 mm dishes of HEK 293 cells were transiently transfected using Effectene Transfection Reagent (Qiagen) according to the manufacturer's protocol and were harvested for patch clamp experiment 48~72 hours later. The SK2 and SK3 clone were developed in our laboratory. HEK 293 cells were transfected with 2.0 μg of *KCNN2*/pIRES-EGFP2 or 2.0 μg of *KCNN3*/pIRES-EGFP2 plasmids, respectively. Single cells were picked and propagated in selection media containing hygromycin 200 μg/ml. Currents were recorded at baseline and after the exposure to 20 nmol/L Lei-Dab 7, followed by addition of 100 nmol/L apamin. The LeiDab7-sensitive current and apamin-sensitive current (in the presence of LeiDab7) were calculated respectively.

Western blot

Western blot was performed in isolated rabbit left ventricular cardiomyocytes. Lowry protein assay was performed before Western blot to guarantee that the protein loadings were identical among lanes. Samples were loaded on SDS-PAGE and transferred to a nitrocellulose membrane. The blot was probed with the following antibodies: anti-K_{Ca}2.2 (SK2) antibody (1:500, APC-028, Alomone, Jerusalem, Israel), anti-CK2α antibody (1:500, ab181734, Abcam, Cambridge, UK), anti-CK2β antibody (1:500, ab201990, Abcam, Cambridge, UK) and anti-SERCA antibody 2A7-A1 (1:1000). Antibody-binding protein bands were quantified with a Bio-Rad Personal Fx phosphorimager (Hercules,CA). The control sample for SK2 was heterologously expressed human isoform of SK2 in cultured HEK 293 cells.

Immunofluorescence confocal microscopy

Both isolated myocytes and ventricular tissues were used for immunofluorescence staining and confocal microscopy. Isolated rabbit ventricular myocytes were fixed with 1% paraformaldehyde for 30 minutes and seeded on the laminin-coated glass slides for at least 1 hour to allow cell attachment. In addition, ventricular tissue samples were fixed with 4% paraformaldehyde for 45 minutes, followed by storage in 70% alcohol for at least 48 hours. The tissue samples were then processed routinely and embedded in paraffin. Tissue sections (5 μm in thickness) were deparaffinized and hydrated by multiple Xylene and ethanol washes.

Slides with either isolated myocytes or ventricular tissue were washed by water and PBS in Tween 20 for at least 3 times. Samples were then permeabilized and blocked in PBS with 3% BSA and 0.2% Triton X-100 for 1 hour. After blocking, slides were incubated with anti-$K_{Ca}2.2$ (SK2) antibody (APC-028, Alomone, Israel) 1:200 diluted in PBS (BSA 1%) at 4ºC overnight. Subsequently, slides were washed 3 times for 5 minutes with PBS and incubated with protein A conjugated with fluorescent dyes (Alexa 488 by Invitrogen, 1:2000) and DAPI for 1 hour. After this step, the slides were again washed 3 times for 5 minutes with PBS followed by mounting with coverslip glasses. The slides were allowed to dry at room temperature and then sealed with nail polish overnight. For comparison, samples from females and males were stained simultaneously.

Confocal images were obtained through a DMI6000 adaptive Focus Automated Inverted Microscope, Leica TCS SP8 FSU (Argon Ion Laser) Spectral Confocal System with HyD super Sensitivity Detection. For comparison of the fluorescence intensities, slides from females and males were microscopically detected at the same day using identical microscopic settings.

Statistics and data analysis

APD_{25} and APD_{80} were optically measured at the level of 25% and 80% repolarization of the AP, respectively. We used APD_{25} to characterize the early phases (phases 1 and 2) repolarization and APD_{80} to represent the entire repolarization (phase 1, 2 and 3). Thus, the differences between APD_{25} and APD_{80} (APD_{80}-APD_{25}) were used to characterize the repolarization at phase 3. APD_{25}/APD_{80} ratio was used as a quantitative measurement of the AP morphology, with a smaller APD_{25}/APD_{80} ratio reflecting greater AP triangulation while a larger APD_{25}/APD_{80} representing AP squaring. Ca_iTD_{25} and Ca_iTD_{80} were used as measures of early and total Ca_i duration, respectively. We also calculated the differences between Ca_iTD and APD (Ca_iTD_{25}-APD_{25} and Ca_iTD_{80}-APD_{80}) to characterize the Ca_i-V_m coupling. We averaged the APD in the region of interests and presented them in the summary data.

Continuous variables were expressed as mean ± S.E.M. Paired Student's t-tests were used to compare two variables from the same rabbit (such as APD_{25} before and after apamin). Unpaired t-tests were used to compare variables between two groups (such as ΔAPD_{25} between females and males). Multiple t-tests were used to compare I_{KAS} current densities between sexes at different membrane potentials. One way or two way ANOVA with the

appropriate post-tests, as indicated in each experiment, were used to compare the means among three or more different variables. A two-sided p value of <0.05 was considered statistically significant.

Results

Isoproterenol activates I_{KAS} in female rabbit ventricles

Consistent with previous studies (Chua *et al.*, 2011), I_{KAS} blockade by apamin only minimally prolonged APD (by <5%) in ventricles from females and males at baseline (Protocol I, Fig. 1). The magnitudes of APD prolongation was not significantly different between males and females. We then tested the effects of I_{KAS} blockade in the presence of isoproterenol in female rabbit ventricles (Fig 2A, Protocol II). The AP exhibited a prominent phase 2 plateau at baseline. Isoproterenol shortened and triangulated the AP. Subsequent apamin administration (with isoproterenol in the recirculation) significantly prolonged APD_{25} (from 29±2 to 40±2 ms, p<0.001) and APD_{80} (from 92±4 to 101±3, p<0.001, Fig 2B and 2C), indicating I_{KAS} activation during isoproterenol perfusion. In addition to APD prolongation, apamin also affected the AP morphology, i.e. reversing isoproterenol induced AP triangulation and restoring the phase 2 plateau of repolarization, by lengthening APD_{25} (11±1 ms and 41±6%) more prominently than APD_{80} (9±1 ms and 10±1 %, p=0.018 for absolute value and p<0.001 for percentage, Fig 2D). As a result, the ratio of APD_{25}/APD_{80} was significantly increased (from 32±2% to 40±2%, p<0.001, Fig 2E). Apamin significantly abbreviated differences between APD_{80} and APD_{25} from 63±2 to 60±3 ms (P=0.043, Fig 2F), indicating a slight acceleration of phase 3 repolarization. Furthermore, as shown in Fig 2G, the prolongation of the entire repolarization (positive ΔAPD_{80}) was associated with the abbreviation of phase 3 repolarization (negative $\Delta(APD_{80}- APD_{25})$) in 7/8 females (dots in quadrant IV), indicating the APD prolongation was completely attributed to the prolongation of phase 2 repolarization. After isoproterenol washout, APD further prolonged towards the baseline level. As shown in Fig. 2H, TMP recording in cardiomyocytes of female rabbits also verified the optical mapping findings. These results indicate that I_{KAS} is activated during β-adrenergic stimulation in female rabbit ventricles.

Ca_i mapping was simultaneously performed in females under Protocol II (Fig. 3). Compared with baseline, isoproterenol markedly shortened Ca_iTD_{25} and Ca_iTD_{80} (Fig. 3A) but increased the peak Ca_i (Fig. 3B). These findings indicate higher Ca_i at phase 2

repolarization. In addition, isoproterenol markedly increased the differences between Ca_iTD and APD (Ca_iTD-APD) and more drastically at Ca_iTD_{25}-APD_{25} than at Ca_iTD_{80}-APD_{80} (30±2 vs. 23±3, p=0.041, Fig. 3C and 3F), suggesting an early activated outward current in compensation for the amplified $I_{Ca,L}$ during phase 2 repolarization.. Apamin had minimal effect on Ca_iTD and peak Ca_i (Fig. 3B and 3D), but resulting in significant abbreviation of Ca_iTD_{25}-APD_{25} (from 30±2 to 20±2 ms, p<0.001, Fig. 3E) and elimination of the isoproterenol-induced differences between Ca_iTD_{25}-APD_{25} and Ca_iTD_{80}-APD_{80} (p=0.563, Fig. 3G). Taken together, isoproterenol increases Ca_i, which in turn activates I_{KAS} to shorten the APD. Therefore, isoproterenol increases the differences between Ca_iTD_{25} and APD_{25} during phase 2 (negative Ca_i-APD coupling).

SK2, but not SK3 or I_{KS}, is responsible for isoproterenol-induced AP triangulation in females

Among subtypes of SK channels which generate I_{KAS}, SK2 and SK3 are important to ventricular repolarization and are completely blocked by 100 nM apamin (Yu *et al.*, 2014). Here, we took advantage of the specific SK2 blocker Lei-Dab7 (20 nmol/L) (Shakkottai *et al.*, 2001) to distinguish the contributions of I_{KAS} conducted by different SK subtypes. Firstly, we verified the selectivity of Lei-Dab7 on SK2 over SK3 (Fig. 4A and 4B). Lei-Dab7 at 20 nmol/L inhibited the majority of whole-cell currents in *KCNN2* transfected HEK293 cells but only had minimal effect on *KCNN3* transfected cells. *KCNN2* channels that have already bound Lei-Dab7 only poorly responded to subsequent apamin, while *KCNN3* current was eliminated by apamin. These results indicate Lei-Dab7 at 20 nmol/L only blocks SK2 channels.

We further tested the effects of Lei-Dab7 (20 nmol/L) in females under Protocol III (Fig. 4). In the presence of isoproterenol, SK2 blockade by Lei-Dab7 significantly prolonged APD_{25} and to a smaller extent APD_{80} (Fig. 4C and 4D). Subsequently administered apamin, which only blocked SK3 with Lei-Dab7 pretreatment, failed to further lengthen APD (Fig. 4E and 4F). In other words, SK2 blockade ($\Delta APD_{LeiDab7\text{-}isoproterenol}$) had significantly larger effects than SK3 blockade ($\Delta APD_{Apamin\text{-}LeiDab7}$) on both APD_{25} (11±1 vs. 1±1 ms, p=0.007) and APD_{80} (13±2 vs. 1±1 ms, p=0.004, Fig. 4G). These results suggest that SK2, rather than SK3, is the predominant channel isoform underlying I_{KAS} activation during β-adrenergic stimulation.

Similar to I_{KAS}, I_{Ks} is also calcium sensitive and is enhanced during sympathetic stimulation (Aflaki *et al.*, 2014; Banyasz *et al.*, 2014; Bartos *et al.*, 2017). To exclude I_{Ks} as a cause of AP triangulation in females, we pretreated ventricles with I_{Ks} blocker chromanol 293B (10 μmol/L) in Protocol IV (Fig. 5). With I_{Ks} blockade, isoproterenol still shortened and triangulated AP. Subsequent apamin administration significantly prolonged APD_{25} and to a lesser extent APD_{80}, indicating that I_{KAS} contributes to APD shortening and AP triangulation independently of I_{Ks}.

I_{KAS} is minimally activated by isoproterenol in male rabbit ventricles

To test sex differences in I_{KAS} activation, we repeated Protocol II in male rabbit ventricles (Fig. 6A). In contrast to females, apamin prolonged APD very slightly after isoproterenol infusion, although the increment was statistically significant (for APD_{25}, from 30±2 to 33±2 ms and for APD_{80}, from 93±3 to 98±4 ms, p=0.001 for both, Fig. 6B and 6C). The prolongation at APD_{25} and APD_{80} were similar (for absolute value: 3±0 ms vs. 4±0 ms, p=0.154; for percentage: 11±0% and 6±1%, p=0.060; Fig. 6D) and barely altered the APD_{25}/APD_{80} ratio (32±2 vs. 33±2, p=0.101, Fig. 6E), indicating no major AP morphology change by apamin. Apamin had little effect on phase 3 repolarization (represented by APD_{80}-APD_{25}, 64±3 vs. 65±4, p=0.180, Fig. 6F). Fig. 6G showed that apamin abbreviated phase 3 repolarization but prolonged the APD_{80} in 4/8 male rabbit ventricles (positive ΔAPD_{80} with negative $\Delta(APD_{80}-APD_{25})$, dots in quadrant IV). These data indicate that the APD prolongation, although only slightly, was completely attributable to phase 2 prolongation in these 4 rabbits. For the other 4 males, however, the APD_{80} prolongation relied on the phase 3 prolongation [positive ΔAPD_{80} with positive $\Delta(APD_{80}-APD_{25})$, dots in quadrant I], which was different apamin responses from females. As shown in Fig. 6H, we further verified the findings of optical mapping at cellular level by TMP recording in cardiomyocytes from male rabbits. Taken together, in contrast to females, males only exhibit minimal I_{KAS} activation both at baseline and during isoproterenol infusion. I_{KAS} activation could shorten either phase 2 or phase 3 repolarization of the AP in males.

To evaluate the mechanism of isoproterenol-induced AP shortening and triangulation which is independent of I_{KAS} activation in males, we pretreated male rabbits with chromanol 293B to inhibit I_{Ks} which is activated by isoproterenol and exhibits stronger activation in males than females (Zhu *et al.*, 2013). As shown in Fig. 7, chromanol 293B prolonged both APD_{25} and APD_{80} and more prominently at APD_{80}. Compared with females, males had

significantly larger APD prolongation, suggesting stronger I_{Ks} activation in males than females. However, isoproterenol still shortened and triangulated APD even with I_{Ks} and subsequent I_{KAS} blockade. These results indicate that isoproterenol-induced APD shortening and triangulation in males cannot be explained only by I_{Ks} and I_{KAS} activation.

The differential I_{KAS} activation after isoproterenol infusion between sexes is summarized in Fig. 8. Females had significantly greater responses to I_{KAS} blockade than males in APD_{25} (for absolute value: 11±1 ms vs. 3±0 ms, p<0.001; for percentage: 39±5% vs. 11±2%, p<0.001; Fig. 7A) and in APD_{80} (for absolute value: 9±1 ms vs. 5±1 ms, p=0.003; for percentage: 10±1% vs. 5±1%, p=0.006; Fig. 7B). Apamin slightly accelerated phase 3 repolarization in females but not in males ($\Delta(APD_{80}- APD_{25})$: -2±1 vs. 0±1 ms, p=0.035, Fig. 7C). The APD_{25}/APD_{80} ratio was significantly larger in females than in males (40±2% vs. 34±2%, p=0.037, Fig. 7D), indicating differential AP morphology changes by I_{KAS} blockade between sexes.

I_{KAS} current densities are higher in females than males

To better understand the mechanisms of the sex differential ventricular I_{KAS} activation, we examined I_{KAS} at cellular levels by performing patch clamp studies in isolated ventricular cardiomyocytes. As shown in Fig. 9A, with free Ca^{2+} concentration of 1 μM, mean I_{KAS} densities were significantly larger in cells from females than males measured at potential >0 mV (at +10mV: 0.35±0.03 vs. 0.19±0.03 pA/pF; at +20 mV: 0.47±0.04 vs. 0.21±0.03 pA/pF; at +30 mV: 0.75±0.05 vs. 0.28±0.05 pA/pF; at +40 mV: 0.98±0.09 vs. 0.34±0.06 pA/pF; p<0.05, respectively). We further tested I_{KAS} densities with pretreatment of 100 nmol/L isoproterenol (Fig. 9B). In the presence of isoproterenol, I_{KAS} densities were significantly larger in myocytes from female than male rabbits at potential >0 mV (at +10mV: 0.42±0.08 vs. 0.13±0.03 pA/pF; at +20 mV: 0.70±0.09 vs. 0.24±0.02 pA/pF; at +30 mV: 0.99±0.10 vs. 0.38±0.03 pA/pF; at +40 mV: 1.30±0.12 vs. 0.51±0.03 pA/pF; p<0.05, respectively). These patch clamp results supported our observations in optical mapping.

SK2 channel protein expressions are higher in females than males

Since SK2 carried the enhanced I_{KAS} by isoproterenol in females, we examined the SK2 channel expressions by western blot and confocal immunofluorescence microscopy in both sexes. Western blotting in Fig. 10A showed that SK2 protein expression was significantly higher in female rabbit cardiomyocytes than in males (SK2 normalized to

SERCA: 0.075±0.005 vs. 0.043±0.004, p=0.003). As further shown in Fig. 10B and 10C, confocal immunofluorescence microscopy detected the expression of SK2 along the Z-line of plasma membrane at higher fluorescence intensities in females than that in males from both isolated cardiomyocytes and ventricular tissue sections. These results indicate that sex differences exist in SK2 protein expressions, which contribute to sex differences in I_{KAS}.

CK2 activities correlate with I_{KAS} suppression in males

Among its participation in a broad range of cellular signaling pathways, CK2 phosphorylates calmodulin, thus lowing the Ca^{2+} affinity of SK2 channels and reducing I_{KAS} in neurons (Pachuau *et al.*, 2014). To evaluate if CK2 activity contributed to I_{KAS} suppression in male rabbit ventricles, we tested the effect of CK2 specific blocker TBB on APD (Protocol V). As shown in Fig. 11A, TBB drastically abbreviated and triangulated APD. Subsequently, apamin significantly prolonged both APD_{25} (from 15±2 to 22±1 ms, p=0.034) and APD_{80} (from 39±2 to 64±4 ms, p=0.045, Fig. 11B and 11C), indicating that CK2 inhibition in males can increase the I_{KAS} activation. Although Western blotting showed CK2α and CK2β had similar expression levels between sexes (Fig. 11D), the significantly higher CK2/SK2 ratio in males than in females (for CK2α/SK2: 12±2 vs. 21±2, p=0.012; for CK2β/SK2 ratio: 11±1 vs. 18±2, p=0.031, Fig. 10E) may correlate with smaller I_{KAS} in males.

Sex differences in I_{KAS} are not secondary to sex differences in $I_{Ca,L}$

SK2 is molecularly coupled with L-type calcium channels (LTCC) (Lu *et al.*, 2007). The magnitude of $I_{Ca,L}$ density is known to be smaller in males than in females (Vizgirda *et al.*, 2002). It is therefore possible that the weaker $I_{Ca,L}$ in males partially explains the lower of I_{KAS}. To test that hypothesis, BayK8644 was used to amplify $I_{Ca,L}$ (Protocol VI, Fig. 12). In males, compared with baseline, BayK8644 led to markedly enlarged Ca_iTD, drastically increased peak Ca_i and prolonged APD. However, subsequently administered apamin failed to further prolong APD, indicating that BayK8644 failed to activate I_{KAS} in males. As a comparison, apamin prolonged APD in the presence of BayK8644 in females. These results are inconsistent with the hypothesis that the sex differences in I_{KAS} are simply secondary to the sex differences in $I_{Ca,L}$.

I_{KAS} blockade eliminates negative Ca_i-V_m coupling at phase 2 and attenuates APD alternans

Cardiac repolarization alternans often precedes life-threatening ventricular arrhythmias. In alternans, Ca_i and V_m are coupled either positively (large Ca_i transient prolongs APD of the same beat) or negatively (large Ca_i transient shortens APD of the same beat) (Kennedy *et al.*, 2017). To test the effects of I_{KAS} on alternans, rapid pacing was performed in females (Protocol VII, Fig. 13). At basal condition, Ca_i-V_m coupling was positive such that alternans was electromechanically concordant. During isoproterenol (Fig. 13A), the Ca_i-V_m coupling was still positive and the alternans remained electromechanically concordant at the level of APD_{80}. However, at early repolarization phases at APD_{25} level, Ca_i-V_m coupling became negative such that alternans became electromechanically discordant. In other words, during phase 2, a larger Ca_i transient (beat 1) led to a shorter and more triangular AP, while a smaller Ca_i transient (beat 2) corresponded to a longer and less triangular AP. As shown in Fig. 13B, I_{KAS} blockade by apamin eliminated the negative Ca_i-V_m coupling and APD_{25} alternans (presented by $\Delta APD_{25,\ beat1\text{-}beat2}$) and also markedly attenuated APD_{80} alternans (presented by $\Delta APD_{80,\ beat1\text{-}beat2}$). Fig. 13C showed that apamin prolonged APD_{25} of beat 1 more prominently than that of beat 2 (13±1 vs. 6±2 ms, p=0.004) while APD_{80} prolongations were similar between the two adjacent beats (5±1 vs. 7±1 ms, p=0.250). Fig. 12D showed that apamin eliminated alternans at APD_{25} (from -7±0 to 0±1 ms, p=0.002) and attenuated alternans at APD_{80} (from 21±1 to 17±1, p=0.010). These results indicate that β-adrenergic stimulation elicits more abundant I_{KAS} activation at phase 2 than at phase 3 repolarization and during beats with a larger Ca_i transient than those with smaller Ca_i transient, leading to negative Ca_i-V_m coupling and electromechanically discordant alternans at early repolarization phases. I_{KAS} blockade mainly prolonged phase 2 repolarization in the beats with larger Ca_i transients and had less effect on the beats with smaller Ca_i transients, resulting in the elimination of negative Ca_i-V_m coupling and electromechanically discordant alternans. As a comparison (Fig. 13E and 13F), in male rabbits, isoproterenol induced Ca_i alternans at PCL 150 ms with less prominent APD alternans. Both Ca_i transient and V_m had little response to apamin. Therefore, the elimination of phase 2 repolarization alternans by I_{KAS} blockade in female rabbits suggests its potential antiarrhythmic effects during β-adrenergic stimulation.

Antiarrhythmic effects of I_{KAS} blockade during isoproterenol infusion

To further assess the antiarrhythmic effects of I_{KAS} blockade during sympathetic stimulation, we compared VF vulnerabilities and characteristics between females and males (Protocol VII, Fig. 14). None of these ventricles developed spontaneous VF. Ventricular fast pacing was therefore performed to induce VF. As shown in Fig. 14A, VF inducibility (the number of induced VF episode) was similar between sexes at baseline, during isoproterenol and after washout. However, VF inducibility after apamin became significantly lower in females than in males. In addition, the first 100 ms at the onset of each episode of VF was optically captured. As shown in the phase map of VF (Fig. 14B), isoproterenol markedly increased the number of PSs in both groups compared with baseline. Apamin prominently decreased the number of PSs in females, but less prominently in males. As summarized in Fig. 14C, the numbers of PSs were similar between sexes at baseline, during isoproterenol and after washout. However, apamin elicited significant lower PS numbers in females than in males. The dominant frequencies were also similar between sexes at baseline. Isoproterenol infusion led to significantly higher dominant frequencies in females than in males. The differences were eliminated by apamin (Fig. 14D). These results indicate that I_{KAS} activation plays important roles in proarrhythmia and VF dynamics during sympathetic stimulation, especially in females.

Discussion

We discovered that β-adrenergic stimulation activates ventricular I_{KAS}. Because sympathetic tone varies throughout the day, the sympathetic sensitivities indicate that I_{KAS} plays a role in modulating ventricular repolarization of normal ventricles. This new finding suggests that I_{KAS} is physiologically important. In addition, sympathetic stimulation unmasks the different I_{KAS} activation profiles between females and males. I_{KAS} activation promotes AP triangulation and ventricular arrhythmias during β-adrenergic stimulation in females while I_{KAS} blockade is antiarrhythmic. Because of the importance of both sympathetic tone and sex differences in cardiac arrhythmogenesis, these findings may be clinically important.

I_{KAS} and sympathetic stimulation

Even in patients without apparent heart diseases, abnormal adrenergic regulation increases the susceptibility to ventricular arrhythmias (Jouven *et al.*, 2005). β-adrenergic activation is

known to regulate cardiac repolarization directly and indirectly via a number of currents including $I_{Ca,L}$ (Reuter, 1983), I_{KATP} (Maruyama *et al.*, 2014), I_{Ks} (Zhu *et al.*, 2013; Aflaki *et al.*, 2014; Bartos *et al.*, 2017), and possibly I_{Kr} (Karle *et al.*, 2002; Harmati *et al.*, 2011) and I_{K1} (Fauconnier *et al.*, 2005; Banyasz *et al.*, 2014). Although increased $I_{Ca,L}$ tends to prolong APD, isoproterenol results in net shortening of APD by activating multiple compensatory outward currents at different phases of repolarization (Harmati *et al.*, 2011; Zhu *et al.*, 2013; Aflaki *et al.*, 2014; Banyasz *et al.*, 2014; Maruyama *et al.*, 2014; Bartos *et al.*, 2017). In addition, as observed in this study and by others (Banyasz *et al.*, 2014), isoproterenol also gave rise to prominent AP morphology changes. While guinea pigs basally exhibited $I_{Kr} > I_{K1} > I_{Ks}$, isoproterenol shaped the AP morphology by reversing the dominance pattern to $I_{Ks} > I_{K1} > I_{Kr}$ (Banyasz *et al.*, 2014). However, the isoproterenol-induced AP triangulation, i.e., preferentially shortening at phase 2 than phase 3 repolarization, is unlikely to rely on I_{Kr}, I_{K1} or I_{Ks} because these voltage dependent currents exhibit limited activation at early repolarization phases under adrenergic stimulation. As an example, in the absence of adrenergic stimulation, I_{Ks} activates slowly during phase 1 and 2 repolarization and reaches its peak at the end of phase 2 (around 0 mV), followed by a rapid decline at phase 3 repolarization. However, in the presence of adrenergic stimulation, the peak of I_{Ks} is postponed from mid plateau to phase 3 repolarization (Banyasz *et al.*, 2014). This was supported by the result that I_{Ks} blockade failed to reverse isoproterenol-induced AP triangulation in this study (Fig. 5 and Fig. 7).

Although weak under basal conditions, I_{KAS} in females was markedly amplified during β-adrenergic stimulation. The I_{KAS} activation happens robustly at the early repolarization phases when $I_{Ca,L}$ activity, sarcoplasmic Ca^{2+} release and Ca_i are all high, resulting in AP triangulation due to more prominent shortening of APD_{25} than APD_{80}. I_{KAS} blockade preferentially prolonged phase 2 repolarization to restore the AP plateau and surprisingly, even slightly shortened phase 3 repolarization, resulting in a squared AP morphology. The AP squaring after I_{KAS} blockade may be attributed to the further I_{Ks} activation facilitated by the longer or perhaps more positive plateau, which subsequently accelerating phase 3 repolarization. These findings indicate possible synergistic action between I_{KAS} and I_{Ks} in AP repolarization during adrenergic stimulation, especially in females. However, due to the results that isoproterenol still shortened and triangulated AP with both I_{KAS} and I_{Ks} blockade in male rabbits, other mechanisms might also contribute in the AP shortening and triangulation, such as the activation of sodium-calcium exchanger

(I_{NCX}) and cAMP-dependent Cl- current ($I_{CFTR-Cl}$) (Perchenet *et al.*, 2000; Zhang *et al.*, 2001; Lin *et al.*, 2006).

Sex differences in SK2 channels

Sex differences are widely present in a variety of cardiac ion currents and exert large influences on cardiac electrophysiological properties and arrhythmogenesis (Liu *et al.*, 1998; Vizgirda *et al.*, 2002; Sims *et al.*, 2008; Zhu *et al.*, 2013). In this study, we found that I_{KAS} also exhibited sex differences but only unmasked during isoproterenol infusion. The activation of I_{KAS} could be attributed to the increased currents conducted by either SK2 or SK3, or both. Our experiments with the selective SK2 blocker Lei-Dab7 suggests that SK2, rather than SK3, is the dominant isoform mediating the enhanced I_{KAS} during sympathetic stimulation. SK2 channel protein had significantly higher expressions in females than in males, thus contributing to the majority of the sex differences in I_{KAS} activation. However, it is known that SK2 and SK3 proteins can form heteromeric channels in atria (Tuteja *et al.*, 2010; Hancock *et al.*, 2015). Therefore, we cannot exclude the possibility that SK2 specific blocker also inhibits I_{KAS} conducted by the heteromerically assembled SK2-SK3 channels in ventricles.

The sex differences in I_{KAS} were also verified by voltage clamp studies showing that outward I_{KAS} densities were larger in isolated ventricular myocytes from females than males with 1 μmol/L intracellular Ca^{2+} at basal condition or in the presence of isoproterenol. Western blot and immunostaining suggested that SK2 protein expressions were increased in females than males. However, similar I_{KAS} densities between sexes were detected at potentials ≤0 mV. Since SK2 channels are known for the versatile function and plasticity, the significant increase in outward I_{KAS} occurring only at potentials >0 mV suggests the mechanism is unlikely to simply result from differences in SK2 protein expressions. The sex-specific differences in outward I_{KAS} could be due to differential sensitivities of SK channels to voltage-dependent block by internal Mg^{2+} or other ions. Another explanation is due to the fixed intracellular Ca^{2+} in the patch clamp study. In intact cardiomyocytes, Ca^{2+} influx and subsequent release through LTCC and ryanodine receptor (RyR) might increase the local subsarcolemmal Ca^{2+} concentration up to 100 μmol/L, while intracellular Ca^{2+} concentration might only reach 1 μmol/L. Since I_{KAS} is very sensitive to local Ca^{2+} between SK channel and LTCC/RyR (Zhang *et al.*, 2018), it is possible that I_{KAS} recorded at a fixed global Ca^{2+}

concentration was not high enough to differentially activate I_{KAS} between sexes. Further studies with dynamical Ca^{2+} fluctuation are needed.

The Ca^{2+} sensitivity of SK2 channels are strongly modulated by CK2 in neurons (Adelman *et al.*, 2012). Heart failure decreases the interaction between CK2 and SK2 and consequently enhances the sensitivity of I_{KAS} to Ca^{2+} (Yang *et al.*, 2015). Consistent with those studies, our results further suggested the potential participation of CK2 inhibition on cardiac I_{KAS} activation. While male rabbit ventricles expressed lower SK2 channels than females, the equally expressed CK2 between sexes resulted in a higher CK2/SK2 ratio in males. While these results might in part contribute to the findings of the present study, more work will be needed to prove a causal relationship between CK2/SK2 ratio and the sex differences of I_{KAS} densities.

Notably, the function of SK channels not only relies on the total protein expression, but also depends critically on the subcellular distribution and the cell-surface membrane expression. Interacting proteins, such as α-actinin and filamin A, regulate SK channel anterograde trafficking to the surface membrane and recycling (Lu *et al.*, 2009; Rafizadeh *et al.*, 2014; Zhang *et al.*, 2017). It is possible that the differential channel trafficking properties exist between sexes and contribute to different I_{KAS} response to sympathetic stimulation.

Antiarrhythmic effects of I_{KAS} blockade

AP triangulation, with either APD abbreviation or prolongation, predicts serious proarrhythmia (Hondeghem *et al.*, 2001). Agents that prolong phase 3 repolarization (triangulation) are proarrhythmic, while agents that prolong phase 2 without slowing phase 3 (squaring) are generally antiarrhythmic (Hondeghem *et al.*, 2001). Thus, it is important to develop repolarization-delaying agents that lengthen APD in the safe fashion. In females, I_{KAS} blockade prolongs phase 2 repolarization without prolonging phase 3 repolarization, reversing AP triangulation and leading to AP squaring, thereby predicting a potential antiarrhythmic effect. Therefore, I_{KAS} could be a promising target for the development of antiarrhythmic agents, especially for females.

Cardiac alternans is a precursor to VF. APD and Ca_i transient alternans are caused by instabilities in both V_m and Ca_i cycling dynamics and their coupling (Weiss *et al.*, 2006). V_m and Ca_i are coupled via calcium sensitive currents, such as $I_{Ca,L}$ (Weiss *et al.*, 2006), I_{NCX} (Weiss *et al.*, 2006), I_{Ks} (Kennedy *et al.*, 2017) and I_{KAS} (Kennedy *et al.*, 2017). *In silico* models in the absence of I_{KAS}, Ca_i and V_m exhibit positive coupling and electromechanically

concordant alternans (Kennedy *et al.*, 2017). After introducing I_{KAS} with a relatively low calcium affinity, APD is shortened when Ca_i transient is large, resulting in negative Ca_i-V_m coupling and electromechanically discordant alternans (Kennedy *et al.*, 2017). In the present study, we have experimentally validated this prediction by demonstrating that I_{KAS} activation by isoproterenol caused Ca_i-V_m coupling to shift from positive to negative, resulting in electromechanically discordant alternans, especially at phase 2 repolarization. I_{KAS} blockade attenuated negative Ca_i-V_m coupling and phase 2 repolarization alternans. In addition, I_{KAS} blockade reduced the VF vulnerability and altered VF dynamics by reducing the number of PSs and dominant frequency, also suggesting its potential antiarrhythmic effects in females.

Study limitations

The optical mapping was performed only on the epicardium. These findings may not be applicable to mid and endocardium due to the transmurally heterogeneous distribution of I_{KAS} (Yu *et al.*, 2015). Due to the unavailability of normal human cardiac tissue, the sex differences of I_{KAS} in human ventricles remains unknown. However, the rabbit is considered as a good animal model for studying sex differences in cardiac ion currents relevant to humans (Salama & Bett, 2014). Isoproterenol also induces AP triangulation in male rabbit ventricles, but apamin failed to normalize the AP morphology. The mechanisms of AP triangulation in males remains unclear.

Conclusions and implications

A variety of cardiac electrical diseases exhibit sexual dimorphism (Salama & Bett, 2014; Antzelevitch *et al.*, 2016). Understanding the arrhythmogenic mechanisms may therefore be important for generating sex-specific therapies. Although ventricular I_{KAS} is relatively small, it still plays important roles in regulating AP under a variety of physiological and pathological conditions. In the present study, we show that adrenergic stimulation causes greater activation of I_{KAS} in females than males. The sex differences of I_{KAS} are attributed to the differences in the expressions and biophysical property of SK2 channels and CK2/SK2 ratios. Activation of I_{KAS} is more abundant during phase 2 than during phase 3 repolarization, leading to AP triangulation, negative Ca_i-V_m coupling, electromechanically discordant phase 2 alternans and increased VF vulnerability. I_{KAS} blockade is potentially antiarrhythmic in females. Drugs specifically targeting cardiac I_{KAS} should be effective and safe. Amiodarone, a commonly used antiarrhythmic drug, is known to suppress I_{KAS} (Turker *et al.*, 2013). More

specific I_{KAS} blockers have also been tested in animal models (Diness *et al.*, 2017; Ko *et al.*, 2018). I_{KAS} blockers may prove to be a new class of antiarrhythmic drugs with sex specific clinical applications.

Additional information

Competing interests

None

Author contributions

MC: design, data acquisition and analysis/interpretation; drafting and revision. DY, SG, DZX and ZW: data acquisition and analysis. ZC, MRL, SFL, THE and JNW: design, interpretation and revision. PSC: conception, design, interpretation; drafting and revision. All authors approved the final version of the manuscript. All authors agree to be accountable for the data integrity and ensuring that questions related to the accuracy or integrity of any part of the work are appropriately investigated and resolved. All persons designated as authors qualify for authorship, and all those who qualify for authorship are listed.

Funding

NIH P01HL78931, R56HL71140; R42DA043391 and TR0022080, a Charles Fisch Cardiovascular Research Award endowed by Dr Suzanne B. Knoebel of the Krannert Institute of Cardiology, a Medtronic-Zipes Endowment and the Indiana University Health-Indiana University School of Medicine Strategic Research Initiative.

Acknowledgements

We thank Nicole Courtney, Jin Guo, Christopher Corr, David Adams, David Wagner and Jian Tan for their assistance.

References

Adelman JP, Maylie J & Sah P. (2012). Small-Conductance Ca^{2+}-Activated K^+ Channels: Form and Function. *Annu Rev Physiol* **74,** 245-269.

Aflaki M, Qi XY, Xiao L, Ordog B, Tadevosyan A, Luo X, Maguy A, Shi Y, Tardif JC & Nattel S. (2014). Exchange protein directly activated by cAMP mediates slow delayed-rectifier current remodeling by sustained beta-adrenergic activation in guinea pig hearts. *Circ Res* **114,** 993-1003.

Antzelevitch C, Yan GX, Ackerman MJ, Borggrefe M, Corrado D, Guo J, Gussak I, Hasdemir C, Horie M, Huikuri H, Ma C, Morita H, Nam GB, Sacher F, Shimizu W, Viskin S & Wilde AA. (2016). J-Wave syndromes expert consensus conference report: Emerging concepts and gaps in knowledge. *Heart Rhythm* **13,** e295-324.

Banyasz T, Jian Z, Horvath B, Khabbaz S, Izu LT & Chen-Izu Y. (2014). Beta-adrenergic stimulation reverses the I_{Kr}-I_{Ks} dominant pattern during cardiac action potential. *Pflugers Arch* **466,** 2067-2076.

Bartos DC, Morotti S, Ginsburg KS, Grandi E & Bers DM. (2017). Quantitative analysis of the Ca^{2+} -dependent regulation of delayed rectifier K^+ current I_{Ks} in rabbit ventricular myocytes. *J Physiol* **595,** 2253-2268.

Chan Y-H, Tsai W-C, Ko J-S, Yin D, Chang P-C, Rubart M, Weiss JN, Everett T, Lin S-F & Chen P-S. (2015). Small conductance calcium-activated potassium current is activated during hypokalemia and masks short term cardiac memory induced by ventricular pacing. *Circulation* **132,** 1377-1386.

Chang PC, Hsieh YC, Hsueh CH, Weiss JN, Lin SF & Chen PS. (2013a). Apamin induces early afterdepolarizations and Torsades de Pointes ventricular arrhythmia from failing rabbit ventricles exhibiting secondary rises in intracellular calcium. *Heart Rhythm* **10,** 1516-1524.

Chang PC, Turker I, Lopshire JC, Masroor S, Nguyen BL, Tao W, Rubart M, Chen PS, Chen Z & Ai T. (2013b). Heterogeneous upregulation of apamin-sensitive potassium currents in failing human ventricles. *J Am Heart Assoc* **2,** e004713.

Chen PS, Chen LS, Fishbein MC, Lin SF & Nattel S. (2014). Role of the autonomic nervous system in atrial fibrillation: pathophysiology and therapy. *Circ Res* **114,** 1500-1515.

Chua SK, Chang PC, Maruyama M, Turker I, Shinohara T, Shen MJ, Chen Z, Shen C, Rubart-von der Lohe M, Lopshire JC, Ogawa M, Weiss JN, Lin SF, Ai T & Chen PS. (2011). Small-conductance calcium-activated potassium channel and recurrent ventricular fibrillation in failing rabbit ventricles. *Circ Res* **108,** 971-979.

Diness JG, Skibsbye L, Simo-Vicens R, Santos JL, Lundegaard P, Citerni C, Sauter DRP, Bomholtz SH, Svendsen JH, Olesen SP, Sorensen US, Jespersen T, Grunnet M & Bentzen BH. (2017). Termination of Vernakalant-Resistant Atrial Fibrillation by Inhibition of Small-Conductance Ca^{2+}-Activated K^+ Channels in Pigs. *Circ Arrhythm Electrophysiol* **10**.

Fauconnier J, Lacampagne A, Rauzier JM, Vassort G & Richard S. (2005). Ca^{2+}-dependent reduction of I_{K1} in rat ventricular cells: a novel paradigm for arrhythmia in heart failure? *Cardiovasc Res* **68,** 204-212.

Hancock JM, Weatherall KL, Choisy SC, James AF, Hancox JC & Marrion NV. (2015). Selective activation of heteromeric SK channels contributes to action potential repolarization in mouse atrial myocytes. *Heart Rhythm* **12,** 1003-1015.

Harmati G, Banyasz T, Barandi L, Szentandrassy N, Horvath B, Szabo G, Szentmiklosi JA, Szenasi G, Nanasi PP & Magyar J. (2011). Effects of beta-adrenoceptor stimulation on delayed rectifier K^+ currents in canine ventricular cardiomyocytes. *Br J Pharmacol* **162,** 890-896.

Hayashi H, Lin SF & Chen PS. (2007). Preshock phase singularity and the outcome of ventricular defibrillation. *Heart Rhythm* **4,** 927-934.

Hondeghem LM, Dujardin K & De Clerck F. (2001). Phase 2 prolongation, in the absence of instability and triangulation, antagonizes class III proarrhythmia. *Cardiovasc Res* **50,** 345-353.

Jouven X, Empana JP, Schwartz PJ, Desnos M, Courbon D & Ducimetiere P. (2005). Heart-rate profile during exercise as a predictor of sudden death. *N Engl J Med* **352,** 1951-1958.

Karle CA, Zitron E, Zhang W, Kathofer S, Schoels W & Kiehn J. (2002). Rapid component I_{Kr} of the guinea-pig cardiac delayed rectifier K^+ current is inhibited by beta1-adrenoreceptor activation, via cAMP/protein kinase A-dependent pathways. *Cardiovasc Res* **53,** 355-362.

Kennedy M, Bers DM, Chiamvimonvat N & Sato D. (2017). Dynamical effects of calcium-sensitive potassium currents on voltage and calcium alternans. *J Physiol* **595,** 2285-2297.

Ko JS, Guo S, Hassel J, Celestino-Soper P, Lynnes TC, Tisdale JE, Zheng JJ, Taylor SE, Foroud T, Murray MD, Kovacs RJ, Li X, Lin SF, Chen Z, Vatta M, Chen PS & Rubart M. (2018). Ondansetron Blocks Wildtype and p.F503L Variant Small Conductance Calcium Activated Potassium Channels. *Am J Physiol Heart Circ Physiol*.

Lee YS, Chang PC, Hsueh CH, Maruyama M, Park HW, Rhee KS, Hsieh YC, Shen C, Weiss JN, Chen Z, Lin SF & Chen PS. (2013). Apamin-sensitive calcium-activated potassium currents in rabbit ventricles with chronic myocardial infarction. *J Cardiovasc Electrophysiol* **24,** 1144-1153.

Lin X, Jo H, Sakakibara Y, Tambara K, Kim B, Komeda M & Matsuoka S. (2006). Beta-adrenergic stimulation does not activate Na^+/Ca^{2+} exchange current in guinea pig, mouse, and rat ventricular myocytes. *Am J Physiol Cell Physiol* **290,** C601-608.

Liu XK, Katchman A, Drici MD, Ebert SN, Ducic I, Morad M & Woosley RL. (1998). Gender difference in the cycle length-dependent QT and potassium currents in rabbits. *J Pharmacol Exp Ther* **285,** 672-679.

Lu L, Timofeyev V, Li N, Rafizadeh S, Singapuri A, Harris TR & Chiamvimonvat N. (2009). Alpha-actinin2 cytoskeletal protein is required for the functional membrane localization of a Ca^{2+}-activated K^+ channel (SK2 channel). *Proc Natl Acad Sci U S A* **106,** 18402-18407.

Lu L, Zhang Q, Timofeyev V, Zhang Z, Young JN, Shin HS, Knowlton AA & Chiamvimonvat N. (2007). Molecular coupling of a Ca^{2+}-activated K^+ channel to L-type Ca^{2+} channels via alpha-actinin2. *Circ Res* **100,** 112-120.

Maruyama M, Ai T, Chua SK, Park HW, Lee YS, Shen MJ, Chang PC, Lin SF & Chen PS. (2014). Hypokalemia promotes late phase 3 early afterdepolarization and recurrent ventricular fibrillation during isoproterenol infusion in Langendorff perfused rabbit ventricles. *Heart Rhythm* **11,** 697-706.

Merri M, Benhorin J, Alberti M, Locati E & Moss AJ. (1989). Electrocardiographic quantitation of ventricular repolarization. *Circulation* **80,** 1301-1308.

Pachuau J, Li DP, Chen SR, Lee HA & Pan HL. (2014). Protein kinase CK2 contributes to diminished small conductance Ca^{2+}-activated K^+ channel activity of hypothalamic pre-sympathetic neurons in hypertension. *J Neurochem* **130,** 657-667.

Perchenet L, Hinde AK, Patel KC, Hancox JC & Levi AJ. (2000). Stimulation of Na/Ca exchange by the beta-adrenergic/protein kinase A pathway in guinea-pig ventricular myocytes at 37 degrees C. *Pflugers Arch* **439,** 822-828.

Rafizadeh S, Zhang Z, Woltz RL, Kim HJ, Myers RE, Lu L, Tuteja D, Singapuri A, Bigdeli AA, Harchache SB, Knowlton AA, Yarov-Yarovoy V, Yamoah EN & Chiamvimonvat N. (2014). Functional interaction with filamin A and intracellular Ca2+ enhance the surface membrane expression of a small-conductance Ca^{2+}-activated K^+ (SK2) channel. *Proc Natl Acad Sci U S A* **111,** 9989-9994.

Reher TA, Wang Z, Hsueh CH, Chang PC, Pan Z, Kumar M, Patel J, Tan J, Shen C, Chen Z, Fishbein MC, Rubart M, Boyden P & Chen PS. (2017). Small-Conductance Calcium-Activated Potassium Current in Normal Rabbit Cardiac Purkinje Cells. *J Am Heart Assoc* **6,** e005471.

Reuter H. (1983). Calcium channel modulation by neurotransmitters, enzymes and drugs. *Nature* **301,** 569-574.

Salama G & Bett GC. (2014). Sex differences in the mechanisms underlying long QT syndrome. *Am J Physiol Heart Circ Physiol* **307,** H640-648.

Shakkottai VG, Regaya I, Wulff H, Fajloun Z, Tomita H, Fathallah M, Cahalan MD, Gargus JJ, Sabatier JM & Chandy KG. (2001). Design and characterization of a highly selective peptide inhibitor of the small conductance calcium-activated K^+ channel, SkCa2. *J Biol Chem* **276,** 43145-43151.

Shen MJ & Zipes DP. (2014). Role of the autonomic nervous system in modulating cardiac arrhythmias. *Circ Res* **114,** 1004-1021.

Sims C, Reisenweber S, Viswanathan PC, Choi BR, Walker WH & Salama G. (2008). Sex, age, and regional differences in L-type calcium current are important determinants of arrhythmia phenotype in rabbit hearts with drug-induced long QT type 2. *Circ Res* **102,** e86-100.

Torrente AG, Zhang R, Wang H, Zaini A, Kim B, Yue X, Philipson KD & Goldhaber JI. (2017). Contribution of small conductance K^+ channels to sinoatrial node pacemaker activity: insights from atrial-specific Na^+ /Ca^{2+} exchange knockout mice. *J Physiol* **595,** 3847-3865.

Turker I, Yu C-C, Chang P, Chen Z, Sohma Y, Lin S-F, Chen P-S & Ai T. (2013). Amiodarone Inhibits Apamin-Sensitive Potassium Currents. *PLoS One* **8,** e70450.

Tuteja D, Rafizadeh S, Timofeyev V, Wang S, Zhang Z, Li N, Mateo RK, Singapuri A, Young JN, Knowlton AA & Chiamvimonvat N. (2010). Cardiac small conductance Ca^{2+}-activated K^+ channel subunits form heteromultimers via the coiled-coil domains in the C termini of the channels. *Circ Res* **107,** 851-859.

Vizgirda VM, Wahler GM, Sondgeroth KL, Ziolo MT & Schwertz DW. (2002). Mechanisms of sex differences in rat cardiac myocyte response to beta-adrenergic stimulation. *Am J Physiol Heart Circ Physiol* **282,** H256-263.

Weiss JN, Karma A, Shiferaw Y, Chen PS, Garfinkel A & Qu Z. (2006). From pulsus to pulseless: the saga of cardiac alternans. *Circ Res* **98,** 1244-1253.

Xu Y, Tuteja D, Zhang Z, Xu D, Zhang Y, Rodriguez J, Nie L, Tuxson HR, Young JN, Glatter KA, Vazquez AE, Yamoah EN & Chiamvimonvat N. (2003). Molecular identification and functional roles of a Ca^{2+}-activated K^+ channel in human and mouse hearts. *J Biol Chem* **278,** 49085-49094.

Yang D, Wang T, Ni Y, Song B, Ning F, Hu P, Luo L, Wang Y & Ma A. (2015). Apamin-Sensitive K^+ Current Upregulation in Volume-Overload Heart Failure is Associated with the Decreased Interaction of CK2 with SK2. *J Membr Biol* **248,** 1181-1189.

Yu CC, Ai T, Weiss JN & Chen PS. (2014). Apamin does not inhibit human cardiac Na^+ current, L-type Ca^{2+} current or other major K^+ currents. *PLoS One* **9,** e96691.

Yu CC, Corr C, Shen C, Shelton R, Yadava M, Rhea I, Straka S, Fishbein MC, Chen Z, Lin SF, Lopshire JC & Chen PS. (2015). Small conductance calcium-activated potassium current is important in transmural repolarization of failing human ventricles. *Circ Arrhythm Electrophysiol* **8,** 667-676.

Zhang HX, Silva JR, Lin YW, Verbsky JW, Lee US, Kanter EM, Yamada KA, Schuessler RB & Nichols CG. (2013). Heterogeneity and function of K_{ATP} channels in canine hearts. *Heart Rhythm* **10,** 1576-1583.

Zhang Q, Timofeyev V, Lu L, Li N, Singapuri A, Long MK, Bond CT, Adelman JP & Chiamvimonvat N. (2008). Functional roles of a Ca^{2+}-activated K^+ channel in atrioventricular nodes. *Circ Res* **102,** 465-471.

Zhang XD, Coulibaly ZA, Chen WC, Ledford HA, Lee JH, Sirish P, Dai G, Jian Z, Chuang F, Brust-Mascher I, Yamoah EN, Chen-Izu Y, Izu LT & Chiamvimonvat N. (2018). Coupling of SK channels, L-type Ca^{2+} channels, and ryanodine receptors in cardiomyocytes. *Sci Rep* **8,** 4670.

Zhang YH, Hinde AK & Hancox JC. (2001). Anti-adrenergic effect of adenosine on Na^+-Ca^{2+} exchange current recorded from guinea-pig ventricular myocytes. *Cell Calcium* **29,** 347-358.

Zhang Z, Ledford HA, Park S, Wang W, Rafizadeh S, Kim HJ, Xu W, Lu L, Lau VC, Knowlton AA, Zhang XD, Yamoah EN & Chiamvimonvat N. (2017). Distinct subcellular mechanisms for the enhancement of the surface membrane expression of SK2 channel by its interacting proteins, alpha-actinin2 and filamin A. *J Physiol* **595,** 2271-2284.

Zhu Y, Ai X, Oster RA, Bers DM & Pogwizd SM. (2013). Sex differences in repolarization and slow delayed rectifier potassium current and their regulation by sympathetic stimulation in rabbits. *Pflugers Arch* **465,** 805-818.

Figure Legends

Figure 1. Effects of I_{KAS} blockade on APD at basal condition. Representative V_m traces, ΔAPD_{25} and ΔAPD_{80} maps in female (**A**) and male (**B**) rabbit ventricles at RA PCL 200 ms, 250 ms and 300 ms under Protocol I. The apamin induced APD prolongation was less than 5% in the absence of β-adrenergic stimulation. Representative V_m traces were obtained at the LV base. **C.** Summary data showed that no significant difference existed in ΔAPD_{25} and ΔAPD_{80} between females and males at baseline (by two-way ANOVA with Sidak's post-test).

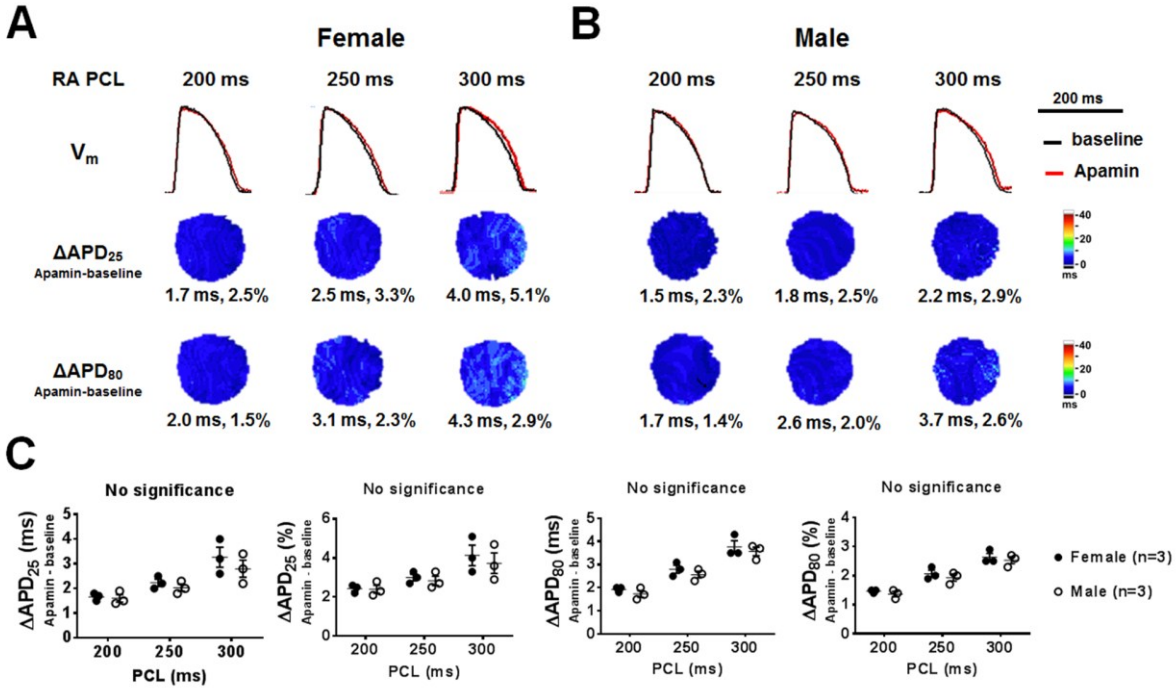

Figure 2. Effects of I_{KAS} blockade on APD during isoproterenol infusion in female rabbit ventricles. **A.** Representative V_m traces, APD_{25}, APD_{80} and APD_{80}-APD_{25} maps at baseline, during isoproterenol, after apamin and after washout (Protocol II). At baseline, the AP exhibited a prominent phase 2 plateau. Isoproterenol markedly shortened APD and more prominently at APD_{25} than at APD_{80}, leading to a short and triangular AP. Representative V_m traces were obtained at the LV base. **B.** Apamin significantly prolonged both APD_{25} and APD_{80} (**C**) and more prominently at APD_{25} (**D**), consequently reversing the AP triangulation and restoring the AP plateau. After washout, the APD further prolonged to the level similar with the baseline. **E.** Apamin significantly increased the ratio of APD_{25}/APD_{80}, resulting in AP squaring and plateau restoration. **F.** Apamin significantly abbreviated APD_{80}-APD_{25}, indicating an acceleration of phase 3 repolarization. Student's paired t tests were performed in C-F. **G.** The prolongation of the total repolarization by apamin (represented by ΔAPD_{80}) corresponded to the shortening of phase 3 repolarization ($\Delta(APD_{80}- APD_{25})$) in 7 out of 8 females (dots in quadrant IV). Therefore, the apamin predominantly lengthened APD_{25}. **H.** Representative TMP recording in ventricular cardiomyocytes from a female rabbit. ISO= isoproterenol.

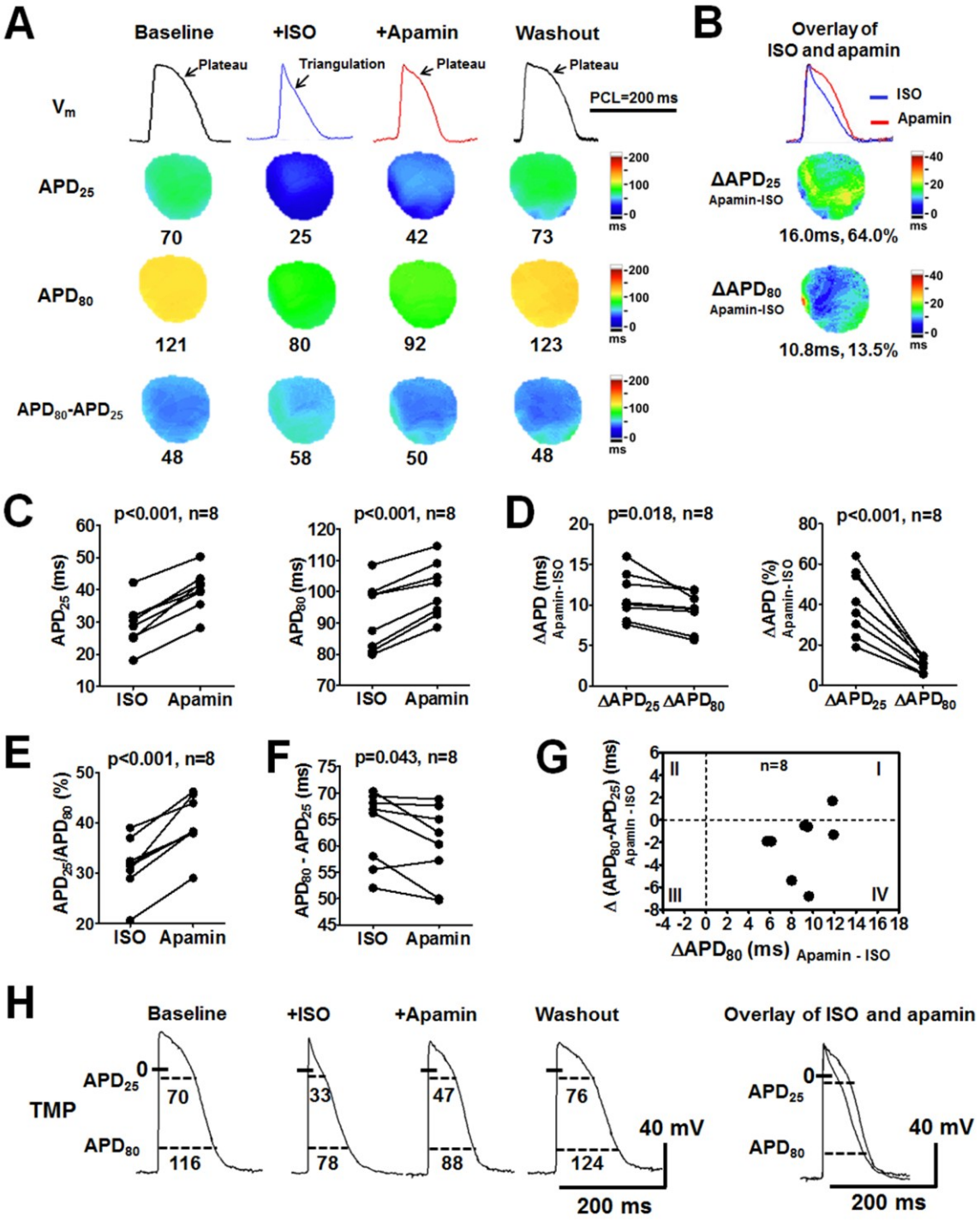

Figure 3. Effects of I_{KAS} blockade on Ca_i and Ca_i-V_m coupling during isoproterenol infusion in females rabbit ventricles. **A.** Representative Ca_i traces, Ca_iTD_{25} and Ca_iTD_{80} maps at baseline, during isoproterenol, after apamin and washout (Protocol II). Compared with baseline, isoproterenol markedly shortened Ca_iTD_{25} and Ca_iTD_{80}. Apamin only slightly prolonged Ca_iTD. After washout, the Ca_iTD prolonged towards the baseline level. Representative Ca_i traces were obtained at the LV base. **B.** Ca_i F/F_0 showed that isoproterenol markedly increased peak Ca_i F/F_0 and accelerated Ca_i upstroke and decay. Apamin had minimal effect on peak Ca_i F/F_0 and Ca_i transient. **C.** Overlapped Ca_i and V_m traces and Ca_iTD-APD maps showed that isoproterenol enlarged the differences between Ca_i and APD compared with baseline, especially at Ca_iTD_{25}-APD_{25}. Apamin markedly attenuated the Ca_iTD_{25}-APD_{25} attributable to the remarkably prolonged APD_{25}. Ca_iTD_{80}-APD_{80} remained similar before and after apamin. Washout further abbreviated Ca_iTD-APD towards baseline. **D.** Apamin had insignificant effect on Ca_iTD_{25} and Ca_iTD_{80}. **E.** Apamin significantly decreased the Ca_iTD_{25}-APD_{25} while had insignificant effect on Ca_iTD_{80}-APD_{80}. **F.** During isoproterenol, Ca_iTD_{25}-APD_{25} was significantly larger than Ca_iTD_{80}-APD_{80}. **G.** After apamin, the differences between Ca_iTD_{25}-APD_{25} and Ca_iTD_{80}-APD_{80} were eliminated. Student's paired t tests were performed in D-G.

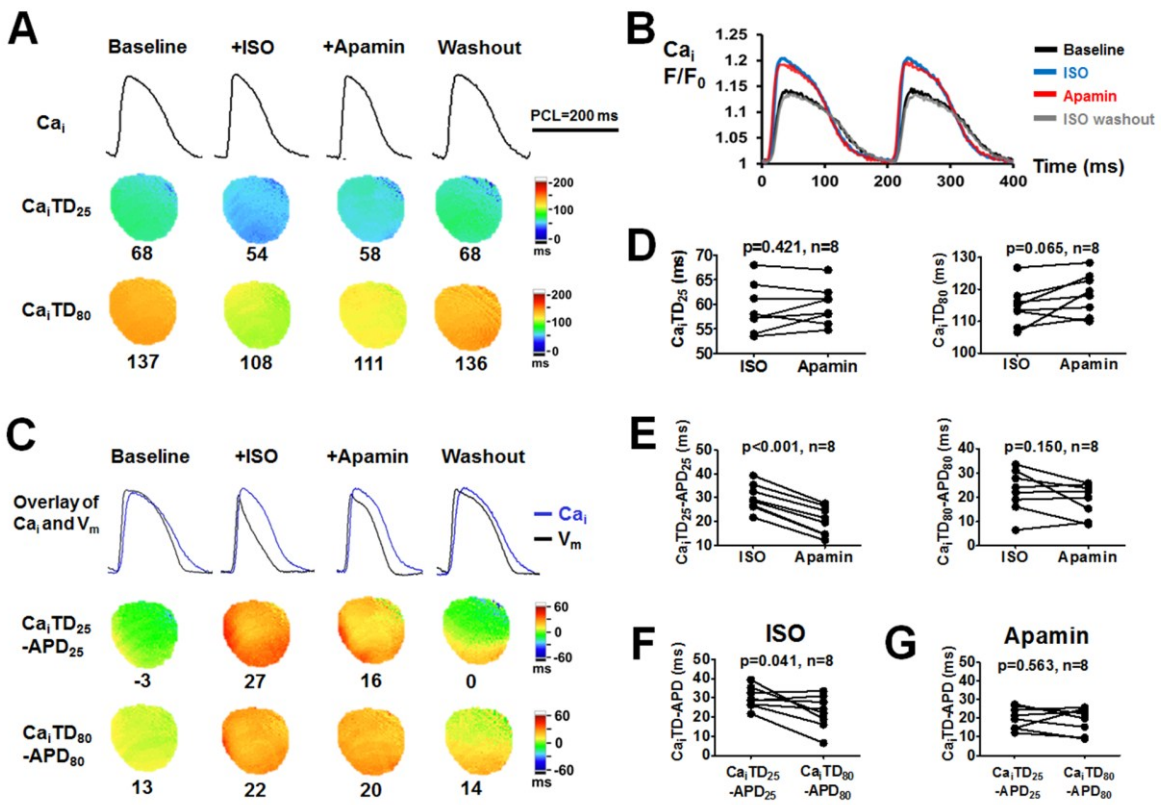

Figure 4. SK2, but not SK3, is responsible for AP triangulation in females. Representative whole cell currents sequentially recorded from *KCNN2* (A) or *KCNN3* (B) transfected HEK293 cells at baseline and in the presence of Lei-Dab7 (20 nmol/L) and subsequent apamin (100 nmol/L). Lei-Dab sensitive current was calculated as the difference between baseline and Lei-Dab7. Apamin sensitive current in the presence of Lei-Dab7 was calculated as the difference between Lei-Dab7 and apamin. C. Representative optical V_m traces, APD_{25} and APD_{80} maps at baseline, during isoproterenol, after Lei-Dab7, after apamin and after washout at PCL 200ms (Protocol III). Representative V_m traces were obtained at the LV base. D. Compared with isoproterenol, Lei-Dab7 prolonged both APD_{25} and APD_{80} and more prominently at APD_{25}, thus leading to the phase 2 plateau restoration. E. Compared with Lei-Dab7, subsequently administered apamin did not further prolong APD. F. Summary data showed that APD_{25} and APD_{80} were significantly longer after Lei-Dab7 and after apamin, both in comparison with those at baseline. APD were similar between Lei-Dab7 and apamin. *$p<0.05$ by one-way ANOVA with Tukey's post-test. G. I_{KAS} conducted by SK2 (represented by $\Delta APD_{LeiDab7\text{-}isoproterenol}$) was significantly more activated than I_{KAS} by SK3 (represented by $\Delta APD_{Apamin\text{-}LeiDab7}$) measured at both APD_{25} and APD_{80} (by Student's paired t-test). ISO= isoproterenol.

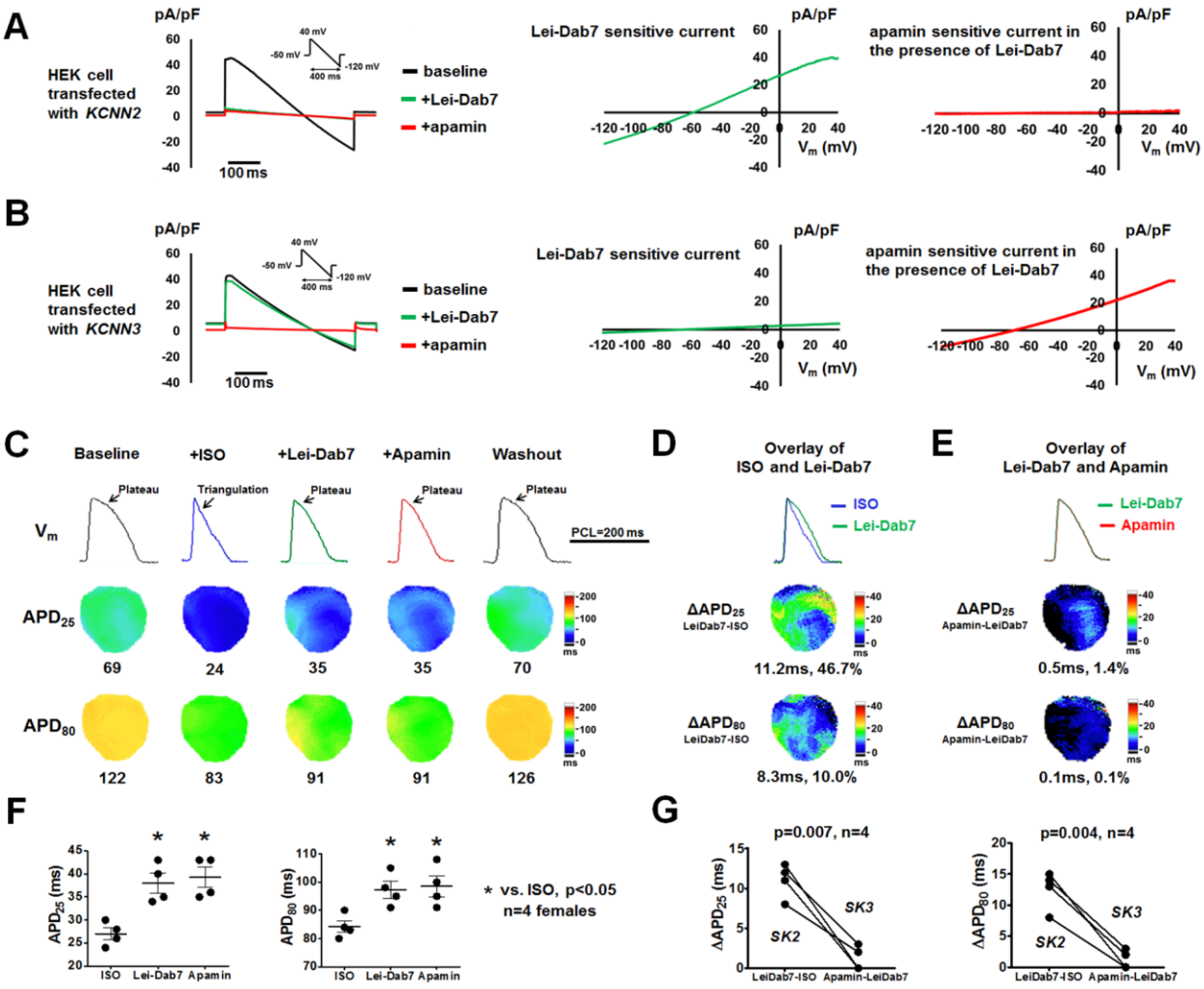

Figure 5. I_{Ks} is not responsible for AP triangulation in females. **A.** Representative V_m traces, APD_{25}, APD_{80} and APD_{80}-APD_{25} maps at baseline, after pretreatment of I_{Ks} blocker chromanol 293B, after isoproterenol, after apamin and after washout (Protocol III). Representative V_m traces were obtained at the LV base. **B.** Compared with baseline, chromanol 293B prolonged APD_{25} and APD_{80} but more prominently at APD_{80} (**D**), by markedly slowing repolarization at phase 3 (APD_{80}-APD_{25}, **E**). With chromanol 293B pretreatment, isoproterenol still shortened and triangulated AP. **C.** Apamin prolonged APD_{25} and APD_{80} (**F**) and more prominently at APD_{25} than at APD_{80} (**G**). Student's paired t tests were performed in D-G.

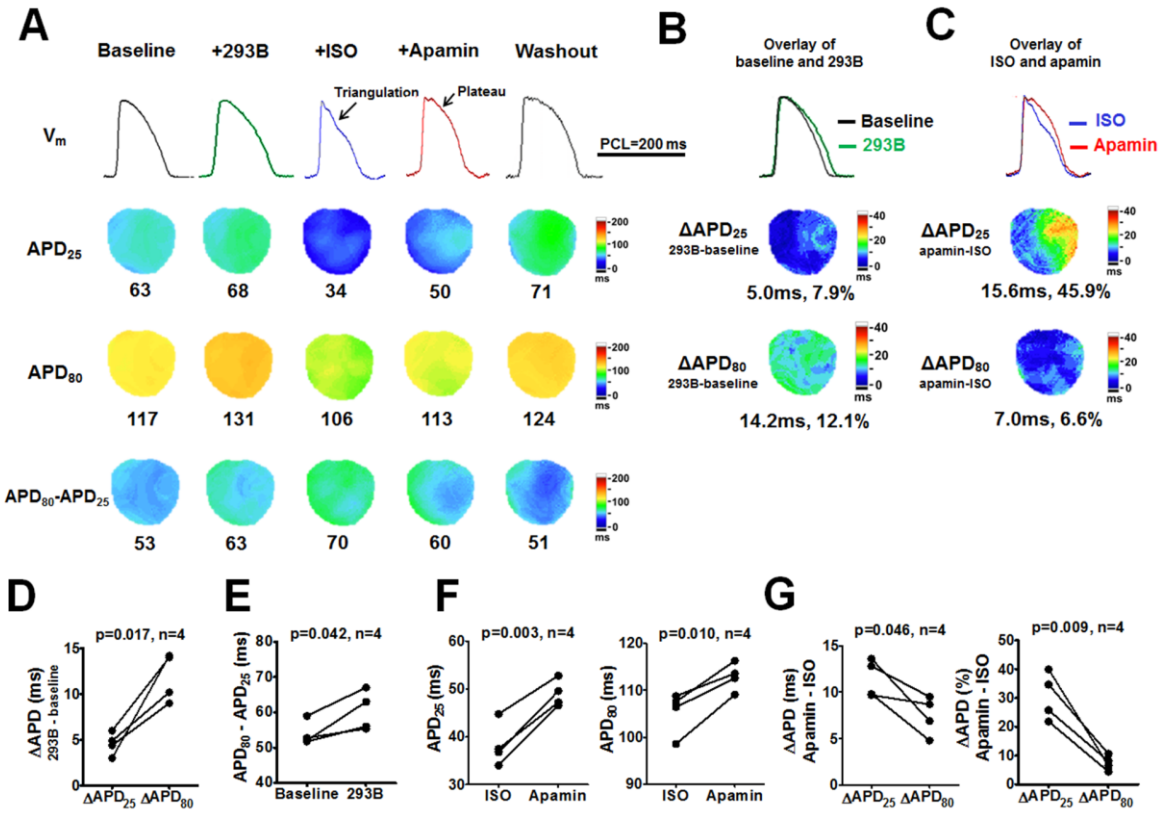

Figure 6. Effects of I_{KAS} blockade on APD during isoproterenol in male rabbit ventricles. **A.** Representative V_m traces, APD_{25} and APD_{80} maps at baseline, during isoproterenol, after apamin and after isoproterenol washout (Protocol II). After isoproterenol, APD was markedly shortened and triangulated. Apamin slightly prolonged APD but did not reverse the AP triangulation. After washout, AP plateau was restored and APD was lengthened towards baseline. Representative V_m traces were obtained at the LV base. **B** and **C.** Apamin prolonged APD_{25} and APD_{80} significantly but only slightly. **D.** Apamin prolonged APD_{25} and APD_{80} to a similar extent. **E.** APD_{25}/APD_{80} ratios were similar before and after apamin. **F.** APD_{80}-APD_{25} were similar before and after apamin. Student's paired t tests were performed in C-F. **G.** APD_{80} prolongation by apamin was partly attributed to phase 3 prolongation in 4/8 ventricles (dots in quadrant I). While in the other 4 ventricles, the APD_{80} prolongation corresponded to slightly phase 3 acceleration (dots in quadrant IV). **H.** Representative TMP recording in ventricular cardiomyocytes from a male rabbit.

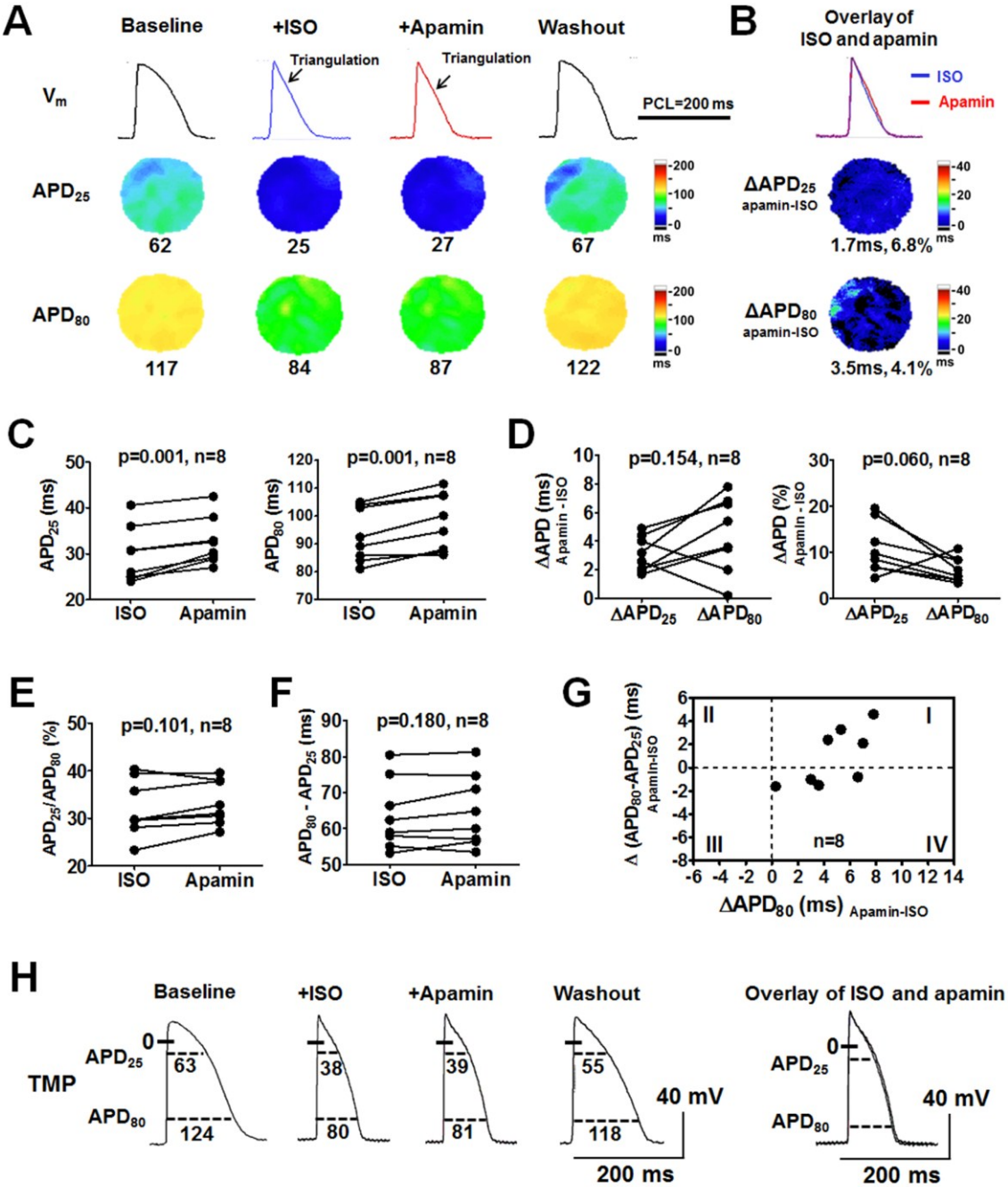

Figure 7. I_{Ks} is not responsible for AP triangulation in males. **A.** Representative V_m traces, APD_{25}, APD_{80} and APD_{80}-APD_{25} maps at baseline, after pretreatment of I_{Ks} blocker chromanol 293B, after isoproterenol, after apamin and after washout (Protocol III). Representative V_m traces were obtained at the LV base. **B.** Compared with baseline, chromanol 293B markedly prolonged APD_{25} and APD_{80} but more prominently at APD_{80}. With chromanol 293B pretreatment, isoproterenol still shortened and triangulated AP. **C.** Apamin only minimally prolonged APD_{25} and APD_{80}. D. Compared with females, males had significant larger response in chromanol 293B-induced APD prolongation (by unpaired t test).

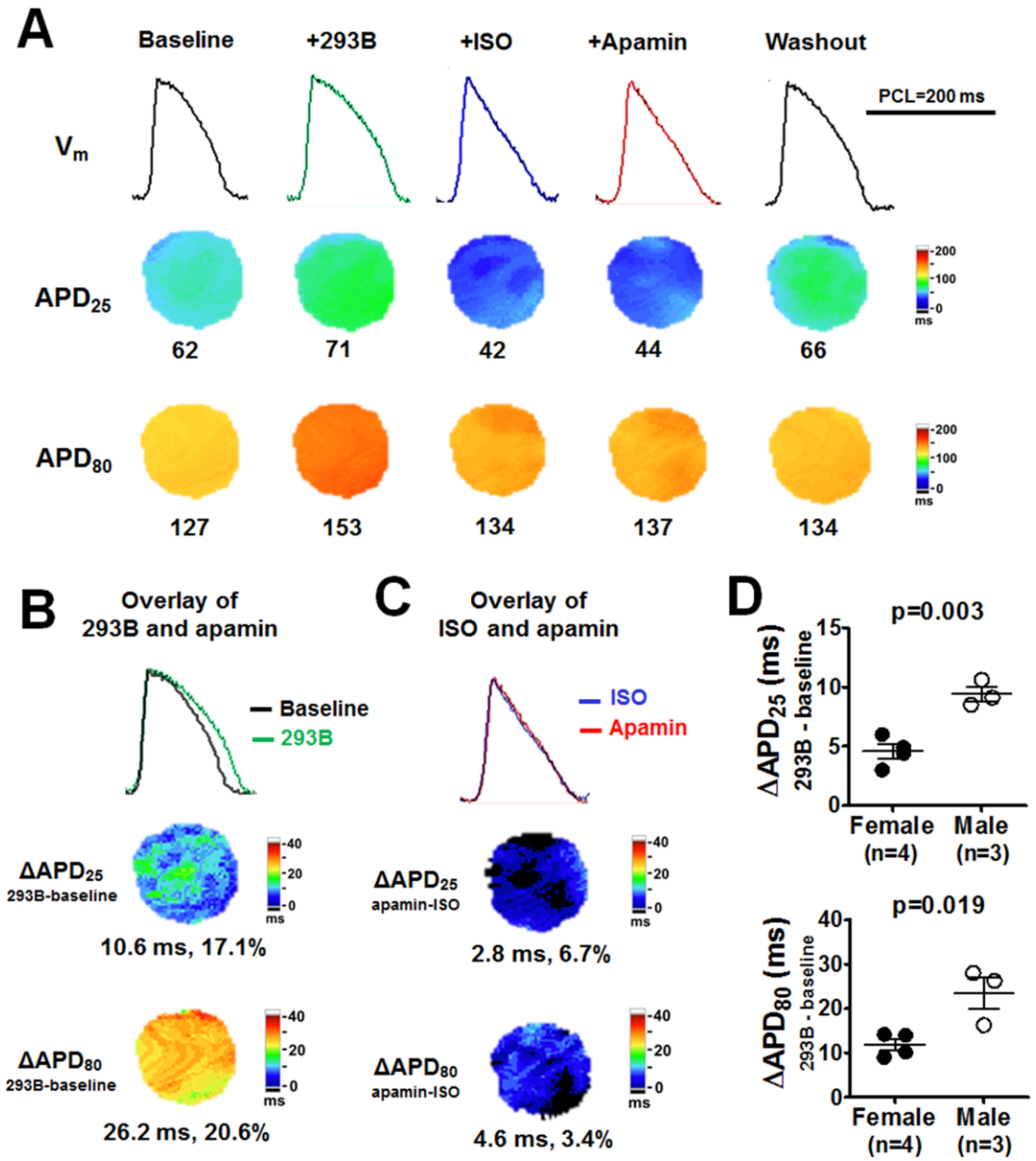

Figure 8. Sex differences on the effects of apamin (Protocol II). In the presence of isoproterenol, female rabbit ventricles exhibited significantly larger apamin-induced prolongation than male rabbit ventricles at both **(A)** APD_{25} and **(B)** APD_{80}. **C.** Females and males responded to apamin significantly differently on phase 3 repolarization ($\Delta(APD_{80}$-$APD_{25})$). Female rabbit ventricles exhibited an abbreviation on $\Delta(APD_{80}$- $APD_{25})$ while male rabbit ventricles did not. **D.** APD_{25}/APD_{80} ratio after apamin was significantly larger in females than in males. Unpaired t-tests were performed in comparison between sexes.

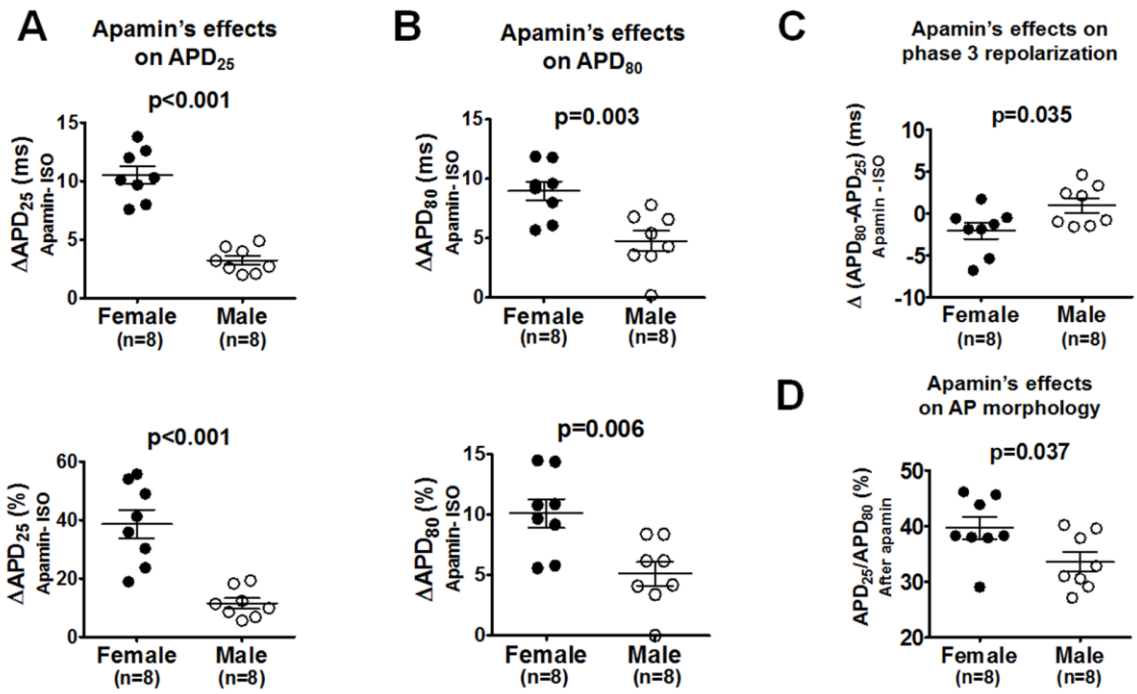

Figure 9. I_{KAS} current density are larger in females than males. I_{KAS} densities of isolated ventricular myocytes by patch clamp using ramp-pulse protocol (test pulse: between +40 and -120 mV; holding potential -70 mV; pulse frequency: every 3 seconds) in the absence (**A**) or presence of isoproterenol (**B**). Left panel: Representative membrane current traces obtained from female (**a**) and male (**b**) rabbit ventricular myocytes. Currents were recorded with an intrapipette free-Ca^{2+} of 1 μmol/L in the absence ($I_{K\text{-baseline}}$ or $I_{K\text{-isoproterenol}}$, blue) and the presence ($I_{K\text{-apamin}}$, red) of 100 nmol/L apamin. Middle panel: amplified images. Right panel: I_{KAS} was calculated as the difference between $I_{K\text{-baseline}}$/ $I_{K\text{-isoproterenol}}$ and $I_{K\text{-apamin}}$. **c.** I_{KAS} density-voltage relationships from female and male rabbit ventricular cardiomyocytes. *p<0.05 by multiple t tests.

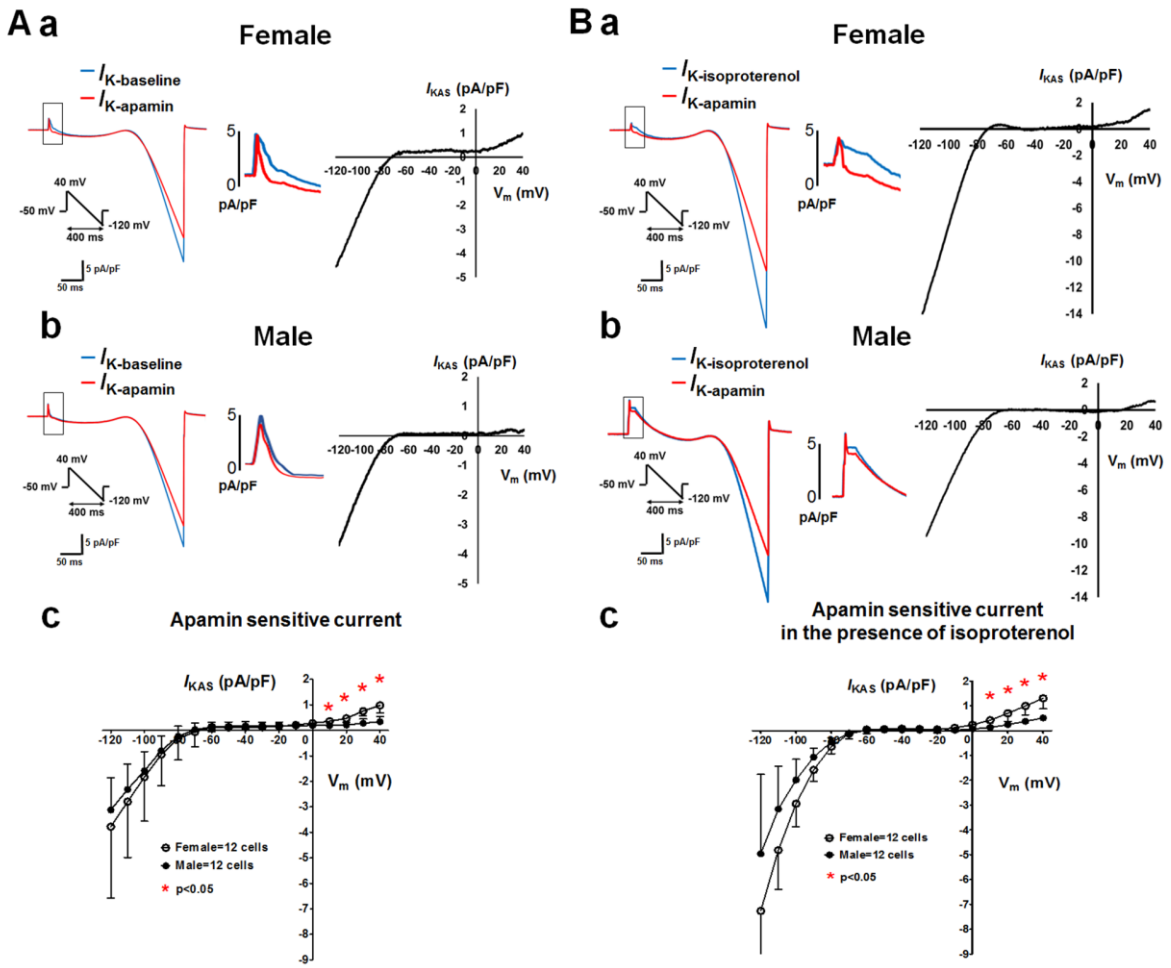

Figure 10. SK2 western blotting and immunostaining of rabbit ventricles. **A.** Western blot showed that SK2 channel protein expression (normalized to SERCA) was significantly higher in females than males (by unpaired t test). hSK2 is heterologously expressed human isoform of SK2 in HEK 293 cells, which serves as the positive control. **B.** Representative confocal immunofluorescence microscopy of SK2 staining in isolated ventricular myocytes. The fluorescence intensity was higher in female than in male ventricular myocytes. The protein A conjugated with Alexa 488 without pretreatment of anti-SK2 antibody was used as a negative control. The fluorescence signals were detected under an identical confocal microscopy setting. a.u.= arbitrary units. **C.** Representative confocal immunofluorescence microscopy of SK2 in left ventricular tissues. The fluorescence signals were stronger in female rabbit ventricular tissues than in males. The fluorescence signals were detected under an identical confocal microscopy setting.

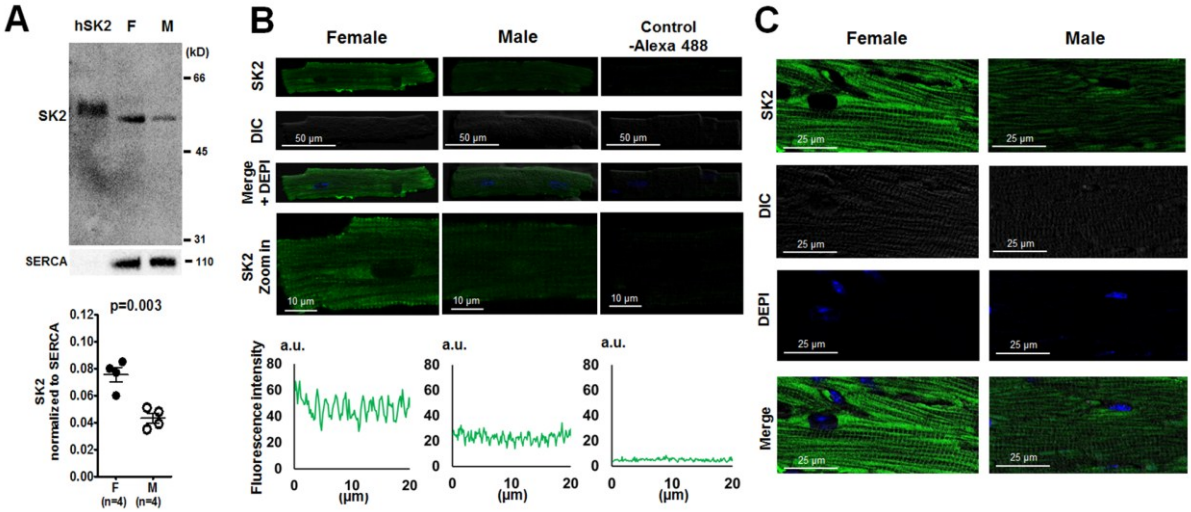

Figure 11. Effects of I_{KAS} blockade during CK2 inhibition in rabbit ventricles. **A.** Representative V_m traces, APD_{25} and APD_{80} maps at baseline, after CK2 inhibitor TBB and after apamin (Protocol V). Compared with baseline, TBB prominently abbreviated APD_{25} and APD_{80}, leading to a short and triangular AP. Apamin significantly prolonged APD_{25} and APD_{80} (**B** and **C**). Representative V_m traces were obtained at the LV base. Student's paired t tests were performed in C. **D.** Western blot showed similar protein expressions of CK2α and CK2β between cardiomyocytes from females and males rabbit ventricles. **E.** Males had significantly higher CK2α/SK2 and CK2β/SK2 ratios than females (by unpaired t test).

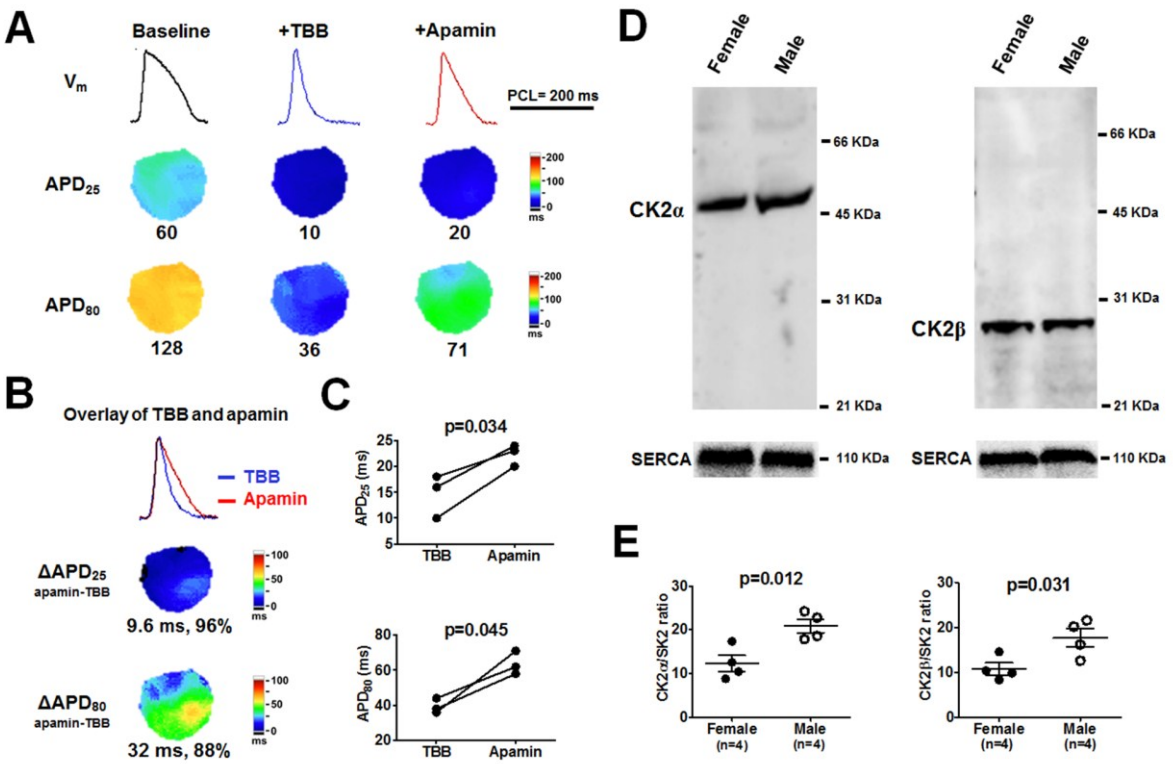

Figure 12. Effects of I_{KAS} blockade during BayK8644 in male (**A-F**) and female (**G-H**) rabbit ventricles. **A.** Representative Ca_i traces, Ca_iTD_{25} and Ca_iTD_{80} maps at baseline, after BayK8644, after apamin and after washout in a male rabbit (Protocol VI). BayK8644 markedly prolonged Ca_iTD_{25} and Ca_iTD_{80} while apamin had minimal effect on Ca_iTD. **B.** The overlapped Ca_i traces and ΔCa_iTD maps showed BayK8644 markedly prolonged Ca_iTD compared with baseline. **C.** BayK8644 markedly increased the peak Ca_i F/F_0. **D.** Corresponding V_m traces, APD_{25} and APD_{80} maps. Compared with baseline, BayK8644 markedly prolonged APD_{25} and APD_{80}. **E.** Apamin only slightly prolonged APD_{25} and APD_{80}. Representative V_m and Ca_i traces were obtained at the LV base. **F.** With BayK8644 pretreatment, apamin prolonged APD_{25} or APD_{80} both insignificantly (by Student's paired t test). **G** and **H.** Representative V_m traces, APD_{25} and APD_{80} maps in a female rabbit (Protocol VI). Compared with baseline, BayK8644 markedly prolonged APD_{25} and APD_{80}. Subsequent apamin administration further prolonged APD_{25} and APD_{80}, and more prominently at APD_{25}. **I.** Female rabbits had significant larger response in apamin-induced APD prolongation than male rabbits with BayK8644 pretreatment (by unpaired t-test).

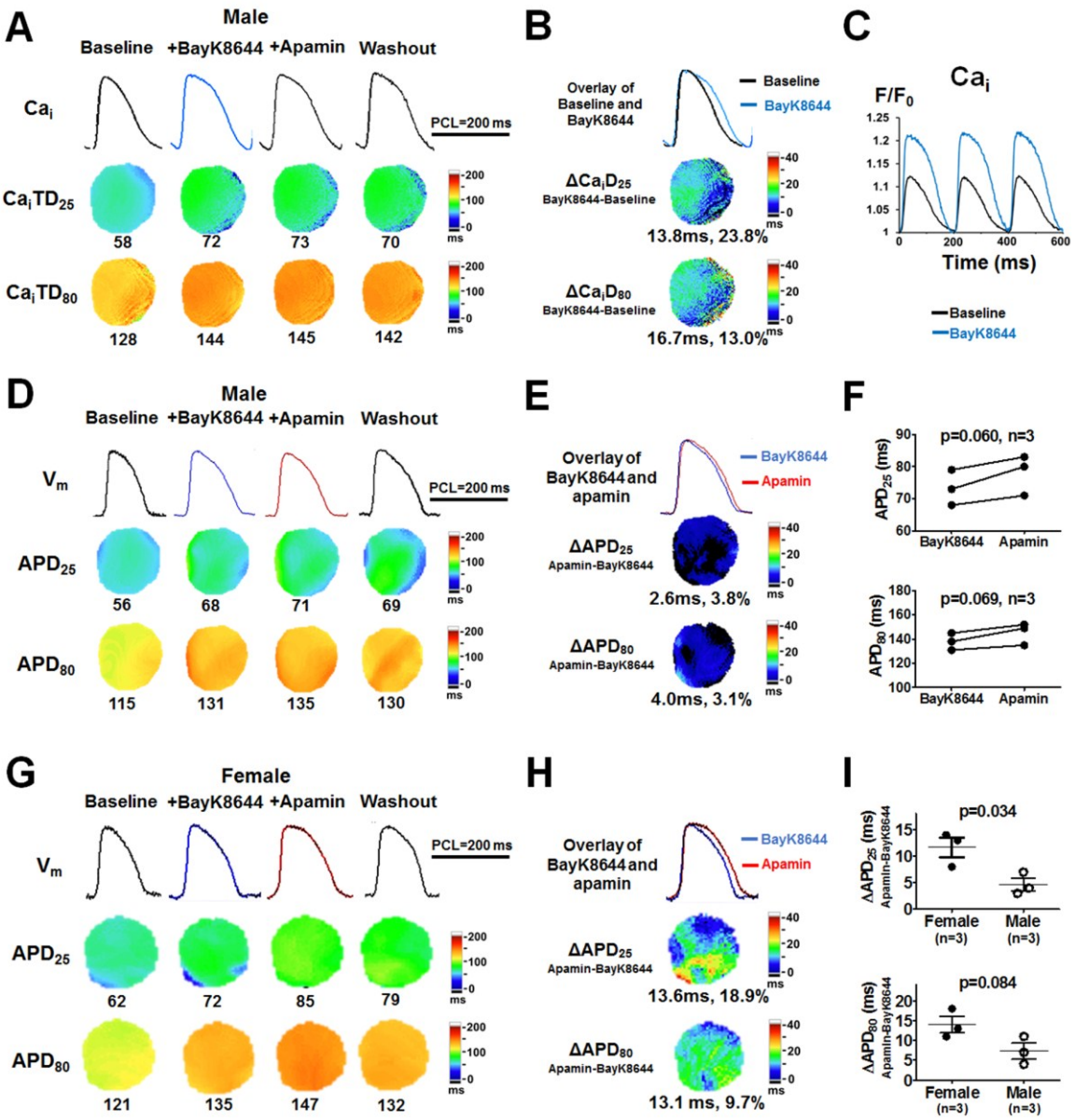

Figure 13. I_{KAS} blockade eliminates negative Ca_i-V_m coupling at phase 2 and attenuates APD alternans in female (**A-D**) but not male (**E-F**) rabbit ventricles (Protocol VII). **A** exhibited electromechanically discordant phase 2 alternans after isoproterenol. Despite the positive Ca_i-APD_{80} coupling, Ca_i and APD_{25} became negative coupled, i.e. larger Ca_i transient (beat 1) shortened APD_{25} while the smaller Ca_i transient (beat 2) corresponded to longer APD_{25}. Notice a more triangular AP (smaller APD_{25}/APD_{80}) in beat 1. **B.** Apamin eliminated APD_{25} alternans and Ca_i-APD_{25} negative coupling ($\Delta APD_{25,\ beat1\text{-}beat2}$, from -7 ms to 0 ms). In addition, apamin did not eliminate but markedly attenuated APD_{80} alternans ($\Delta APD_{80,\ beat1\text{-}beat2}$, from 21 ms to 16 ms). **C.** Apamin prolonged APD_{25} of beat 1 more prominently than that of beat 2. The prolongation of APD_{80} was similar between beat 1 and beat 2. **D.** Apamin eliminated APD_{25} alternans ($\Delta APD_{25,\ beat1\text{-}beat2}$) and attenuated APD_{80} alternans ($\Delta APD_{80,\ beat1\text{-}beat2}$) both significantly (by Student's paired t tests). **E** and **F**. In male rabbits, isoproterenol induced Ca_i alternans at PCL 150 ms without prominent APD alternans. Both Ca_i transient and V_m had little response to apamin. L=larger Ca_i transient or longer APD; S=smaller Ca_i or shorter APD.

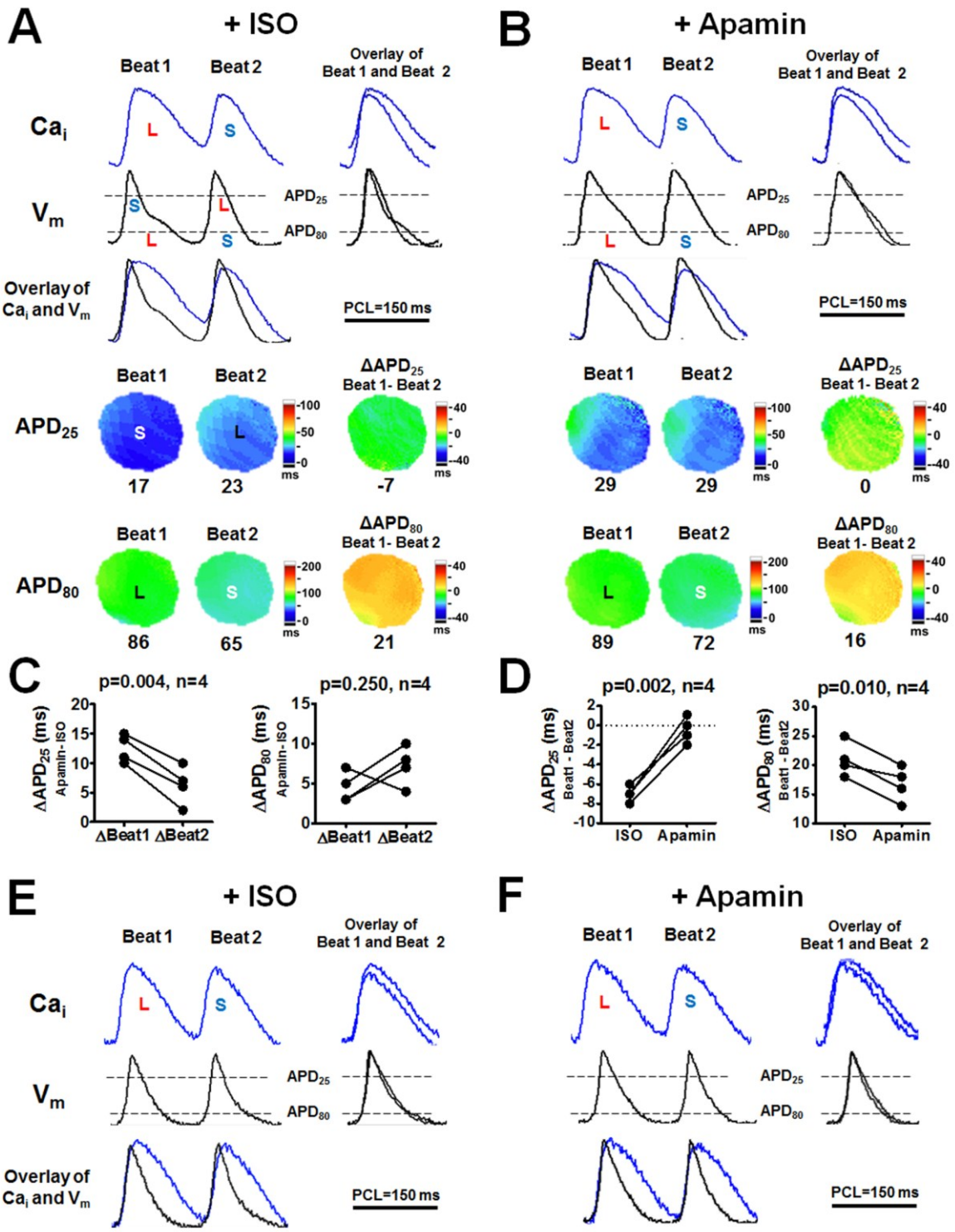

Figure 14. Effects of I_{KAS} blockade on VF inducibility and VF dynamics. **A.** The numbers of induced VF episodes were similar between females and males at baseline, during isoproterenol and after washout. After apamin, however, the numbers of induced-VF episodes became significantly lower in females than in males. VF inductions were attempted 10 times at baseline and after each treatment. **B** exhibited representative phase maps of the first 100 ms of VF after the onset at baseline, after isoproterenol, after apamin and after washout in females (upper panel) and males (bottom panel) (Protocol VII). Compared with baseline, isoproterenol markedly increased the numbers of phase singularities (PSs, black arrowhead) in both groups. Apamin prominently decreased PSs in females, but the effect was less prominent in males. After washout, the numbers of PSs in all three groups were similar with those at baseline. **C.** The numbers of PSs were similar between sexes at baseline, after isoproterenol and after washout. After apamin, however, the numbers of PSs became significantly lower in females than that in males. **D.** VF dominant frequencies were similar between sexes at baseline. After isoproterenol, dominant frequency became significantly higher in females than in males. Apamin eliminated the isoproterenol-induced differences in dominant frequency between sexes. After washout, the dominant frequencies remained similar in females and males. *p<0.05 by two-way ANOVA with Sidak's post-test.

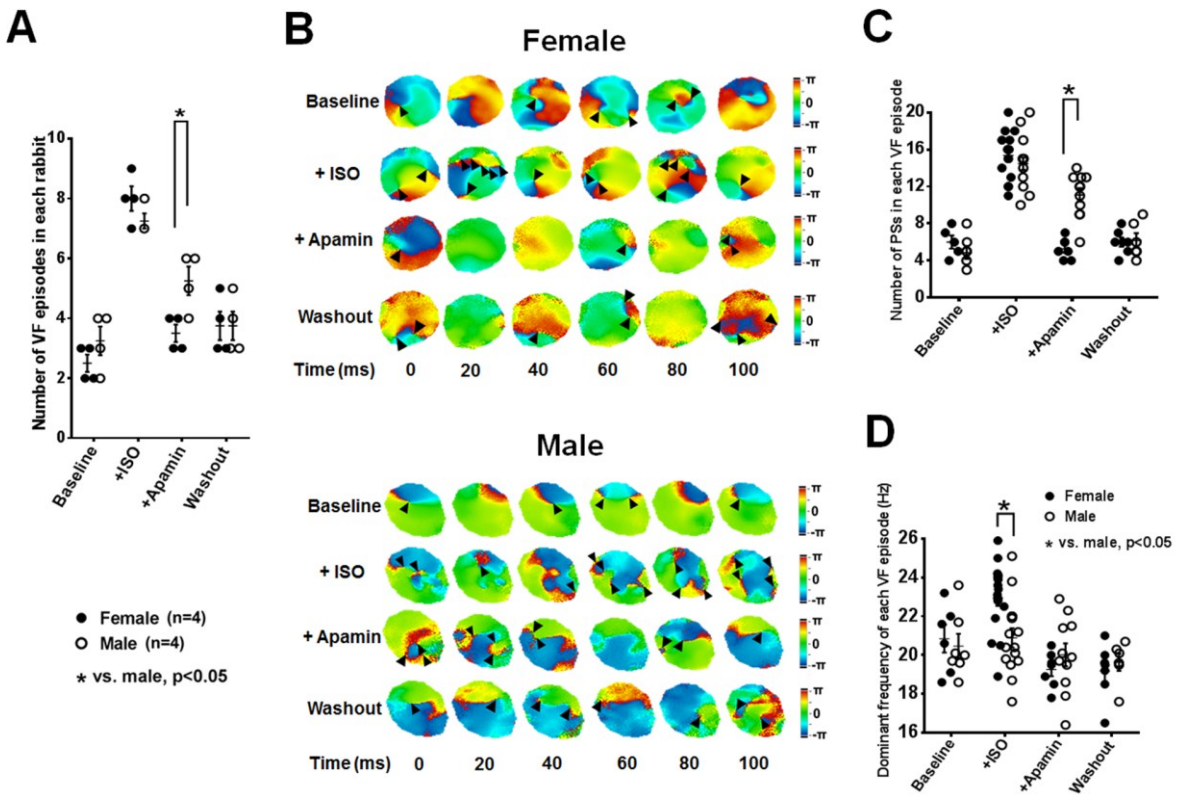

Mu Chen received his MD from Shanghai Jiao Tong University and did resident training at Xinhua Hospital Shanghai. He now works as a Postdoctoral Fellow under the supervision of Dr Peng-Sheng Chen in Krannert Institute of Cardiology, Indiana University. His studies focus on the cardiac small conductance calcium-activated potassium channel and its regulation on ventricular repolarization and arrhythmias.